Sedimentary Geology 445 (2023) 106330

Contents lists available at ScienceDirect

Sedimentary Geology

journal homepage: www.elsevier.com/locate/sedgeo

A bio-chronostratigraphic study of the upper Miocene from the northern Caltanissetta Basin, Sicily (core 3AGN2S04). Implications for dating the Messinian Salinity Crisis onset

Athina Tzevahirtzian [a,*,1], Antonio Caruso [a,1], Federico Andreetto [b], Sergio Bonomo [c], Wout Krijgsman [b]

[a] Dipartimento di Scienze della Terra e del Mare (DiSTeM), Università degli Studi di Palermo, via Archirafi 20, 90123 Palermo, Italy
[b] Paleomagnetic Laboratory "Fort Hoofddijk", Dept. of Earth Sciences, Utrecht University, Budapestlaan 17, 3584, CD, Utrecht, the Netherlands
[c] Istituto Di Geologia Ambientale E Geoingegneria – CNR, Piazzale Aldo Moro, 7, 00185 Roma, RM, Italy

ARTICLE INFO

Article history:
Received 18 October 2022
Received in revised form 13 January 2023
Accepted 15 January 2023
Available online 24 January 2023

Editor: Dr. Catherine Chagué

Keywords:
Messinian Salinity Crisis
(pre-)evaporites
Cyclostratigraphy
Timing
Caltanissetta Basin
Sicily

ABSTRACT

The late Miocene deposits from core 3AGN2S04, located in the northern Caltanissetta Basin (Sicily), display the pre-Messinian Salinity Crisis (MSC) and the MSC events. The present study describes the entire core in terms of lithology, biostratigraphy and magnetostratigraphy and aims to enlighten the relationship between MSC evaporite cyclicity and astronomical forcing. The lithological and micro−/macro-paleontological descriptions document the MSC record, with Stage 1 (onset and Calcare di Base member), Stage 2 (Messinian Erosional Surface) and part of Stage 3 (Upper Gypsum and Lago Mare). Detailed micro-fossil analyses of the pre-evaporites reveal several biostratigraphic events that permit correlations to the well-dated Mediterranean planktonic foraminiferal biostratigraphic zonation of the late Tortonian and Messinian. An integrated bio-cyclostratigraphic analysis allows bed-to-bed correlations of core 3AGN2S04 with the reference sections of Falconara/Gibliscemi (Sicily) and Sorbas (Spain), but also with various other sections from the Caltanissetta Basin. Our cyclostratigraphic correlations show a stratigraphical gap in the core between the late Tortonian Terravecchia Formation and the pre-evaporitic Messinian Tripoli Formation. This hiatus is probably related to the tectonically active geological setting of the northern Caltanissetta Basin. Finally, we show that the repercussions of the paleoenvironmental evolution towards evaporitic deposition and the MSC onset seem to have been diachronous throughout the various perched basins on Sicily characterized by different paleobathymetries. In particular, the onset of the Calcare di Base took place around 40–100 ka before the deposition of the first gypsum bed of the Primary Lower Gypsum units.

1. Introduction

During the Late Miocene, geodynamic and climatic forcings led to the progressive isolation of the Mediterranean and the establishment of restricted environmental conditions causing a large-scale deposition of evaporites (Hsü et al., 1978), the so-called 'SaltGiant'. Numerous successions recording the Mediterranean evolution were studied to better understand the processes that triggered the Messinian Salinity Crisis (MSC) and to refine its chronology. The introduction of cyclostratigraphy as an astronomical dating tool, integrated with bio- and magnetostratigraphic studies applied to the lower Messinian deposits and MSC evaporites (Hilgen et al., 1995; Hilgen and Krijgsman, 1999; Hilgen et al., 1999) resulted in an accurate chronostratigraphic framework for the MSC. This led to the conclusion that the MSC was a relatively short event of about 640 kyr (Krijgsman et al., 1999a, 1999b) and took entirely place in the reverse Chron (3r) of the Gilbert Epoch (Gautier et al., 1994). It is commonly accepted that the MSC ended at 5.332 Ma (Van Couvering et al., 2000; Andreetto et al., 2021), but the timing of the MSC onset is still a matter of debate. High-resolution cyclostratigraphic correlations of sections from the Sorbas Basin (SE Spain) in the western Mediterranean, the Caltanissetta Basin (Sicily, Italy) in the central-southern Mediterranean and Gavdos Island (Greece) in the eastern Mediterranean dated the MSC onset synchronously across the Mediterranean at ~5.96 ± 0.02 Ma (Krijgsman et al., 1999c). A refined age calibration at 5.971 Ma, correlating the first gypsum bed in both Spain (Sorbas Basin) and Italy (Vena del Gesso Basin), three precessional cycles above the base of C3r, was later proposed (Manzi et al., 2013). Alternatively, a diachronous response to the MSC onset was reported by Rouchy and Caruso (2006) in the various

* Corresponding author.
E-mail address: athina.tzevahirtzian@unipa.it (A. Tzevahirtzian).
[1] New address - Dipartimento di Scienze e Tecnologie Biologiche, Chimiche e Farmaceutiche (STeBiCeF), Università degli Studi di Palermo, via Archirafi 18, 90,123, Palermo, Italy.

https://doi.org/10.1016/j.sedgeo.2023.106330
0037-0738/

perched-basins of Sicily, dated between 6.14 and 6.03 Ma, based on the age of the first evaporitic limestone. Zachariasse and Lourens (2021) also suggested a diachronous MSC onset throughout the Mediterranean, respectively dated at 5.97 Ma in Sorbas (SE Spain) and Monticino (N. Italy), both based on the age of the first respective gypsums, while earlier at 6.00 Ma in Gavdos Island (GR) and Falconara (Sicily) based on the age and origin of the first respective evaporitic limestones.

The Caltanissetta Basin is a key area for the MSC, where Messinian outcrops are among the best exposed and most complete (Bellanca et al., 2001; Manzi et al., 2009). Based on observations and onland sections, several stratigraphic models were proposed and refined over the years (e.g. Decima and Wezel, 1971, 1973; Decima et al., 1988; Butler et al., 1995; Garcia-Veigas et al., 1995; Krijgsman et al., 1999a, 1999b, 1999c; Rouchy and Caruso, 2006; Manzi et al., 2009; Roveri et al., 2014). Decima and Wezel (1971) proposed a stratigraphic model with two evaporite units, the Lower Evaporites (LE) and the Upper Evaporites (UE), separated by an erosional unconformity, which they related to an intra-Messinian tectonic event. Later, the unconformity was correlated to the Messinian Erosional Surface (MES), observed in seismic profiles of the western Mediterranean (Cita and Ryan, 1978), and linked to the main Messinian drawdown (Hsü et al., 1973; Lofi et al., 2005). The MES in the Caltanissetta Basin is generally recognized as an angular discordance reflecting a major sedimentological and hydrological change (e.g. Rouchy and Caruso, 2006). The LE comprises the Calcare di Base, the Lower Gypsum (massive selenite of the Cattolica Fm.) and the Salt unit. The UE (or Pasquasia Fm.) is represented by the cyclic occurrence of gypsum (*balatino* and selenite) and marls, overlain by the Arenazzolo siliciclastic sediments. In the initial model of Decima and Wezel (1971), the Salt lies above the Lower Gypsum, whereas Garcia-Veigas et al. (1995) and Rouchy and Caruso (2006) proposed instead a lateral transition between Salt, Lower Gypsum and Calcare di Base suggesting a partially synchronous deposition of different facies in basinal, marginal and sill settings. The model by Roveri et al. (2014) suggests three evolutionary stages of the MSC. In Stage 1 (5.97 to 5.60 Ma - MSC Onset), the Primary Lower Gypsum (PLG) is deposited in shallow water basins; in Stage 2 (5.60 to 5.55 Ma), resedimented evaporites (mainly halite and gypsum) are deposited in deep basins accompanying the maximum sea-level drawdown and; in Stage 3 (5.55 to 5.33 Ma), the Upper Gypsum (UG) has been divided into 2 sub-stages, stage 3.1 (from 5.65 to 5.42 Ma), in which Upper Evaporites are emplaced and stage 3.2 (from 5.42 to 5.33 Ma), also known as Lago Mare stage.

The Caltanissetta Basin was previously studied at high-resolution, focusing on the pre-evaporitic Tripoli Formation that provides evidence of depositional changes up to the base of the "Calcare di Base" member (CdB; Caruso, 1999; Bellanca et al., 2001; Blanc-Valleron et al., 2002; Caruso et al., 2015). The Tripoli Formation is, however, often faulted and incomplete due to the active tectonism of the area (i.e. Falconara, Monte Gibliscemi, Marianopoli, Torrente Vaccarizzo, Serra Pirciata etc.) (Caruso et al., 2015 and reference therein). Moreover, no section has ever provided a reliable and continuous magnetostratigraphic record, due to secondary normal magnetization (Langereis and Dekkers, 1992) or controversial results (Gautier et al., 1994; McClelland et al., 1997). The main part of the MSC concerns, among others, the environmental deposition and timing of the CdB deposition in marginal basins. It is also central to the discussion of whether the CdB marks the MSC onset and whether it is partly a lateral equivalent of the PLG unit (Rouchy and Caruso, 2006) or resedimented LG (Roveri et al., 2014). The youngest units (UG) of the MSC and the Pliocene reflooding are well represented at the Eraclea Minoa section located in the southern Sicilian coast, where the Zanclean Global Boundary Stratotype Section and Point (GSSP) and the Miocene/Pliocene boundary have been defined (Van Couvering et al., 2000).

In the present study, we describe the late Tortonian to late Messinian (~8–5.5 Ma) succession of core 3AGN2S04 from the northern margin of the Caltanissetta Basin, in terms of lithology, biostratigraphy and magnetostratigraphy. A significant stratigraphic gap between the late Tortonian Terravecchia Formation and the Messinian Tripoli Formation in this core was previously documented (Tzevahirtzian et al., 2022). A comparison between core 3AGN2S04 and other sections located throughout the Caltanissetta Basin permits to evaluate the sedimentary influence of the Sicilian-Maghrebian Fold and Thrust (SFTB) system in the northern Caltanissetta Basin. In addition, the influence of astronomical climate forcings on core 3AGN2S04 is investigated. A cyclostratigraphic correlation between sections located in different perched sub-basins allows to better frame the MSC chronostratigraphy and to transcribe the paleoenvironmental and paleogeographic changes of the studied area.

2. Geological setting of the Caltanissetta Basin

The evaporitic successions of the MSC were accumulated within a series of wedge-top basins located in the Caltanissetta Basin (central Sicily) (Fig. 1a). These basins were formed during Neogene times and are characterized by several depocenters and intrabasinal highs, related to the Messinian active thrusting synclines (Butler et al., 1995; Catalano et al., 2013).

The Caltanissetta Basin corresponds to the main depocenter of the Sicilian-Maghrebian foreland basin system and is currently located between the northern Sicilian-Maghrebian chain (Sicani and Madonie Mts.) and the southern SFTB (Fig. 1a). The evolution of Caltanissetta Basin is linked to the Mid (Late)-Miocene opening of the southern Tyrrhenian Sea (Kastens and Mascle, 1990) and to the thrusting and shortening of the Sicilian-Maghrebian chain (Malinverno and Ryan, 1986; Patacca et al., 1990; Doglioni, 1990; Facenna et al., 2001) that progressively formed the southward migrating SFTB. This front advanced about 50 km southwards and south-eastwards between the Early Pliocene and Early Pleistocene (Roure et al., 1990; Catalano et al., 2000; Di Grande and Giandinoto, 2002). SI.RI.PRO seismic profiles have illustrated the regional setting by a foreland monocline that underlies the entire fold and thrust belt and a NNW synformal inner platform characterized by a deeply eroded and uplifted chain evolving southwards to a thinning orogenic wedge (Catalano et al., 2013). Today, the Caltanissetta Basin embodies a complex morpho-structural background from paleogeographic domains of the oceanic realm of Neotethys (Sengör, 1979) and the Africa continental paleo-margin (Bianchi et al., 1987; Roure et al., 1990; Bello et al., 2000).

3. Stratigraphic setting

In the northern Caltanissetta Basin, the Tortonian - Messinian Transition is represented in the more proximal parts of the basin by the Terravecchia Formation and in the more distal parts by the Licata Fm. The Terravecchia Formation consists of three major lithofacies, respectively from bottom to top: i) reddish polygenic conglomerate (TRVa) with clasts of sandstone, Mesozoic limestone and metamorphic rocks; ii) gray-blue, weakly cemented, quartz-sands (TRVb); and, iii) marly and/or silty brown clays (TRVc) (Fig. 1b). These sediments have been deposited on the inner and outer shelf domains, progressively decrease towards the outer wedge-top depozones (Fig. 1b) (Gugliotta, 2012), and constitute a deltaic environment sourced from the rising orogenic belt in the north (Catalano, 1979; Grasso and Pedley, 1988, 1989). The clastic TRVa unconformably overlie the Castellana Sicula Formation (SIC) (Fig. 1b). During this time-interval, marine fossiliferous marls of the Licata Formation were deposited as heteropic passage in bathyal areas. The early Messinian Tripoli Formation overlies the Terravecchia and the Licata formations (Fig. 1b and c), characterized by 49 cycles made of marls, red laminites and diatomitic beds and deposited between 7 to ~6 Ma (Hilgen and Krijgsman, 1999).

The Tripoli Formation is followed by the "Calcare di Base" (CdB) member. Most authors (Caruso et al., 2015; Perri et al., 2017; Gindre-Chanu et al., 2020; Borrelli et al., 2020; Tzevahirtzian et al., 2022) argue that the CdB consists of a 'microbial boundstone' commonly

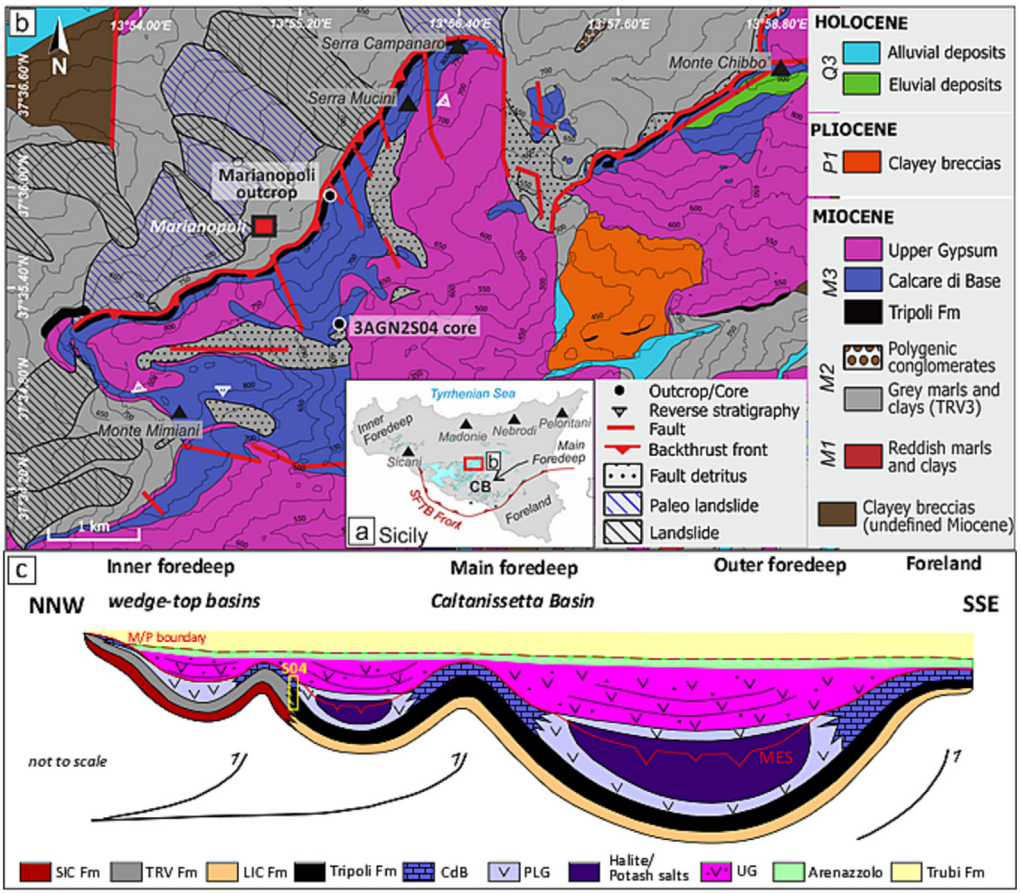

Fig. 1. (a) Location of core 3AGN2S04 in the Caltanissetta Basin, Sicily. (b) Geological map of core 3AGN2S04 (modified after l'Ente Zolfi Italiani, Servizio Geologico Italiano). The isolines correspond to the present-day topography of the area and have been produced using the onshore digital elevation model produced using Copernicus data and information funded by the European Union EU-DEM layers (www.eea.europa.eu). (c) Schematic geologic cross section across the Caltanissetta Basin showing the Tortonian and Messinian deposits (modified after Roveri et al., 2006). SIC Fm: Castellana Sicula Formation; TRV Fm: Terravecchia Formation; LIC Fm: Licata Formation; CdB: Calcare di Base member; PLG: Primary Lower Gypsum; UG: Upper Gypsum; M/P boundary: Miocene/Pliocene boundary. The white rectangle corresponds to the stratigraphic position we assign to the study core 3AGN2S04. From Tzevahirtzian et al. (2022).

observed as 'autobrecciated' due to the interplay of diagenesis and brecciation processes and formed in situ. The CdB corresponds to the Lower Evaporites (LE) unit, and therefore marks the MSC onset (i.e. Decima and Wezel, 1971; Rouchy and Caruso, 2006). The total duration of the LE was estimated ~350–370 kyr in Italy (Hilgen et al., 2007). The CdB member varies between 4 and 10 carbonate-marl (or carbonate-shale) cycles (Caruso et al., 2015) and is partly coeval with the 16 precession-driven cycles of gypsum-marls alternations, known as Primary Lower Gypsum (PLG) (Krijgsman et al., 2001; Rouchy and Caruso, 2006). As implied in the consensus model (Roveri et al., 2014), the PLG is thought to be deposited subaqueously and exclusively in silled basins shallower than 200 m deep (Lugli et al., 2010). Recent studies, however, questioned the necessity of the presence of a topographic sill and the 200 m depth limit of the PLG formation (Ochoa et al., 2015; Raad et al., 2021; Natalicchio et al., 2021; Pellegrino et al., 2021; Meijer, 2021; Raad et al., 2022). According to Butler et al. (1995) and Rouchy and Caruso (2006), the PLG pass laterally into basinal gypsum laminites, halite and K- and Mg-rich potash salts. This sedimentary model is not supported by some authors (Roveri et al., 2008a, 2008b; Lugli et al., 2010; Manzi et al., 2011) that do not consider the CdB as a lateral equivalent of the PLG unit. They subdivided the CdB in three distinctive units of different lithology, age and depositional environment. CdB1 mainly contains sulfur-rich deposits formed in post-MES times. CdB2 comprises in situ formed dolomitic limestones that formed pre-MES and correspond to Stage 1. CdB3 is composed of brecciated limestones that are considered to reflect reworking and therefore linked to Stage 2 (Resedimented Lower Gypsum). CdB type 1 and 3 are thus both of them located after the MES (post 5.60 to 5.55 Ma).

In the most recent MSC stratigraphic framework (Roveri et al., 2014), the UG unit or Gessi di Pasquasia Fm. (Decima and Wezel, 1971) overlies the MES and corresponds to Stage 3, subdivided in 3.1 (UG) and 3.2 ('Lago-Mare'). In the reference section of Eraclea Minoa (Sicily), the UG unit comprises 7 gypsum–marl couplets thought to reflect precession-driven wet-dry cycles (Hilgen et al., 2007; Manzi et al., 2009). Only in Eraclea Minoa, Paratethyan ostracods indicative of brackish and shallow-water conditions are present in the marl beds starting from UG cycle 3 (Grossi et al., 2015; Andreetto et al., 2022). The UG unit was deposited in approximately 175 kyr (Hilgen et al., 2007) and is overlain by the siliciclastic Arenazzolo sediments. The whole succession is topped by the Zanclean Trubi Formation, which marks the re-establishment of normal marine conditions, as the result of the "Zanclean reflooding" of the Mediterranean by Atlantic waters after reopening the connection at Gibraltar (Ruggieri and Sprovieri, 1978; Cita and Colombo, 1979; Kontakiotis et al., 2016; Sciuto and Baldanza, 2020; Bulian et al., 2022a).

4. Material and methods

4.1. Description of core 3AGN2S04

Core 3AGN2S04 was drilled in 2019 by the Italian State Railway Group engineering firm *Italferr*, in the northern area of the Caltanissetta

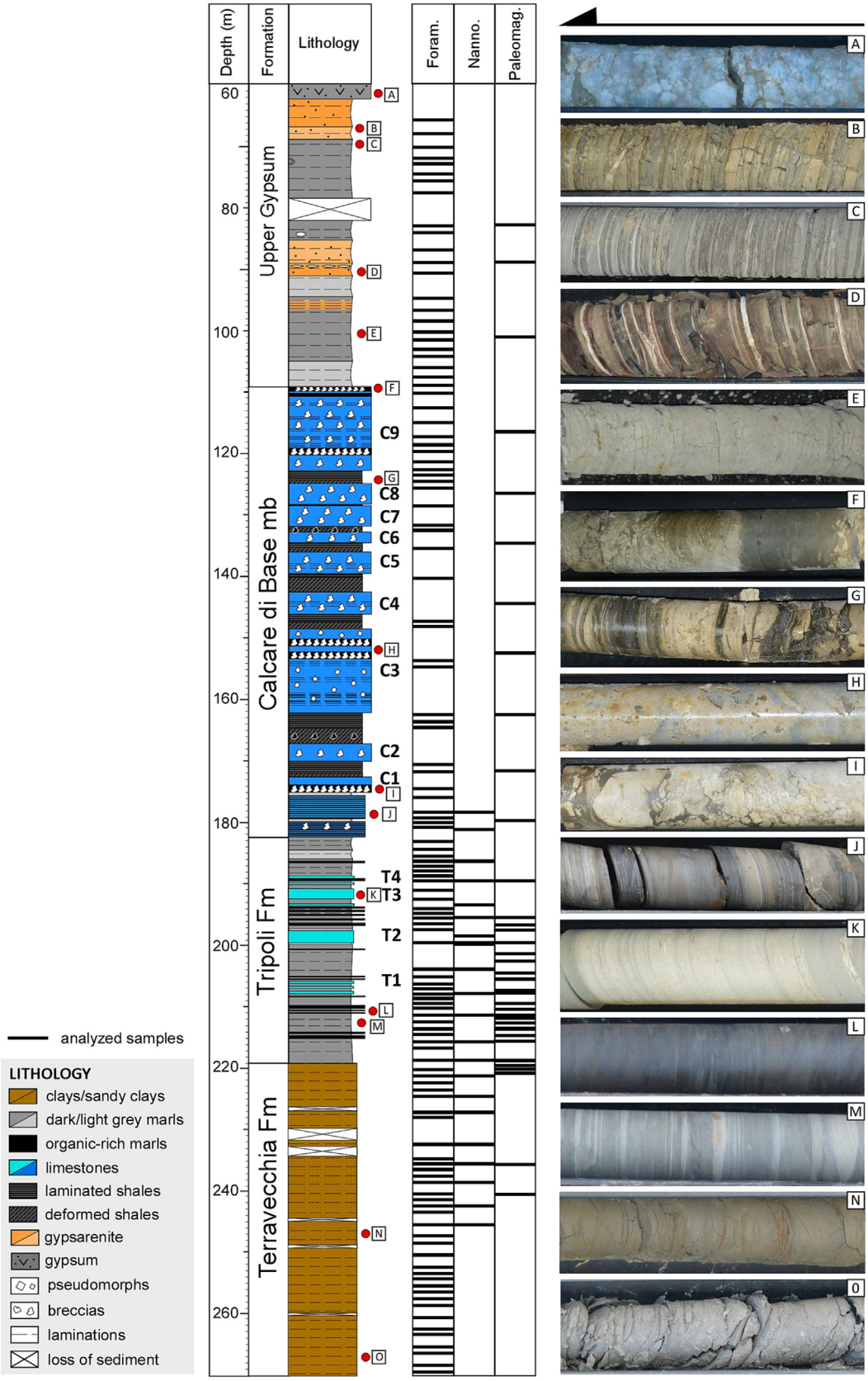

Fig. 2. Detailed lithological log of core 3AGN2S04, core photos (noted A to O and positioned to the core by a red dot) and position of the samples analyzed for micropaleontological (foraminifera and calcareous nannofossils) and magnetostratigraphic studies.

Basin, 3 km south of the town of Marianopoli (Fig. 1b), along the SP42 road coming from the town of San Cataldo (37°35′12.6"N 13°55′31.4″ E). The core is 270 m long. Depths are shown in meters below ground surface.

Core description in terms of mineralogy, isotopic composition, organic matter and petrography was previously performed for the interval 270 to 110 m by Tzevahirtzian et al. (2022), and part of the classical evaporitic succession of the 'Gessoso-Solfifera' Group of Sicily was recognized, comprising from bottom to top:

i) the late Tortonian Terravecchia Formation (270 to 220 m): composed of about 50 m of silty to sandy brownish claystones (Fig. 2), it records a river-dominated deltaic environment, extremely influenced by the dismantling of the northern Maghrebian-Sicilian chain. Sediment loss during core recovery does not permit to describe the core between 226.25 and 227.0 m, 228.0 and 232.0 m, 233.0 and 234.30 m, 235.0 and 235.35 m, 244.65 and 245.0, 249.0 and 249.40 m (Fig. 2);
ii) the Messinian and pre-MSC upper Tripoli Formation (220 to 182 m): composed of diatomaceous marlstones that, from 215 m, contain more frequent and thicker layers of dark gray to black-colored silty mudstones rich in organic matter (Fig. 2). Higher up, organic-rich silty marls alternate with diatomites and gray marls. Thin beds of carbonate appear in the upper part and become thicker (Fig. 2). Between 205 and 207 m, three cm-thick layers of carbonates (T1) emerge, in which thin diatomites and organic-rich marls are embedded. Upwards, two m-thick carbonate beds occur, respectively T2 at 198 m and T3 at 192 m, with, in between, several layers of black marls rich in organic matter. Around 190 and 188 m, cm-thick carbonate beds appear (T4). Around 187 m, organic matter content becomes more significant and brecciated facies starts to appear. The Tripoli Fm of the core records the progressive deterioration of marine conditions and the establishment of a shallow, restricted environment marked by the disappearance of biodiversity and the microbial mediated formation of thin carbonate beds between diatomaceous marls;
iii) the "Calcare di Base" (CdB) member (182 to 110 m): composed of nine thick carbonate beds (C1 to C9) that alternate with organic rich shales (Fig. 2). C1 is a fine-grained carbonate bed, while beds C2 to C9 have a brecciated aspect in which organic-rich shales are embedded (see Tzevahirtzian et al., 2022 for more details regarding the carbonate facies and their origin). The CdB member marks the MSC onset and corresponds to carbonate and shale alternations that reflect climate and sea-level variations (Fig. 2). The carbonate beds record periods of microbial mediated carbonate precipitation under anoxic and evaporitic conditions, while organic-rich shales record periods of anoxic and more humid conditions. One sedimentary cycle includes the repetition of i) fine-grained or laminated carbonates, ii) brecciated carbonates, iii) brecciated shales, iv) laminated shales. Further, the formation of the CdB carbonate beds has been interpreted as the result of syndiagenetic and brecciation processes.

The last carbonate bed (C9) is capped from 110 to 60 m by deposits (Fig. 2) that are described for the first time in this study and that we tentatively assign to the Upper Gypsum unit. No core recovery has been possible above 60 m.

4.2. Biostratigraphy

4.2.1. Foraminifera and ostracods

For the present study, 118 samples were analyzed, 97 between 238 and 110 m and 21 samples in the upper part of the core from 110 to 60 m (Fig. 2). For both, fifty grams of dried sediment were washed through a 63 μm sieve and the residual fraction was oven-dried at 50 °C. The identification of the foraminiferal bio-events was based on a semi-quantitative study of the fraction >63 μm following the biostratigraphic scheme proposed by Lirer et al. (2019). A quantitative analysis has been performed in 38 samples of fraction >125 μm. 39 samples from the Tripoli Formation permitted to observe foraminiferal fluctuations that were compared with the respective intervals of the reference sections of Sorbas – Abad marls (Spain, Sierro et al., 2001) and Falconara – Tripoli Fm (Sicily, Hilgen and Krijgsman, 1999; Blanc-Valleron et al., 2002). The identification of the ostracods in the Upper Gypsum unit has been based on the taxonomy proposed by Stoica et al. (2013, 2016).

4.2.2. Calcareous nannofossils

A qualitative analysis of the calcareous nannofossils was carried out on 26 samples (Fig. 2), in order to recognize the bio-events, using a transmitted light microscope at 1000× magnification. Standard rippled smear slides were prepared, without any chemical treatment, sieving or centrifuging. Separate analyses were also performed to evaluate the abundance of reworked specimens, which included taxa from different stratigraphic intervals (e.g. Eiffellithaceae, Watznaueriaceae, *Nannoconus* spp., *Fasciculithus tympaniformis*, *Helicosphaera walbersdorfensis*, *Sphenolithus heteromorphus*). Calcareous nannofossil taxa were determined using the taxonomy proposed by Perch-Nielsen (1985) and Bown et al. (2004) and following the biostratigraphic scheme for the Mediterranean area proposed by Raffi et al. (2003).

4.3. Magnetostratigraphy

Nineteen levels were sampled along the core and oriented with top-bottom criteria (Fig. 2). The core was not oriented with respect to the north, so only inclination can be used to determine the magnetic polarities. Samples were demagnetized in the paleomagnetic laboratory Fort Hoofddijk at Utrecht University. Thermal demagnetization was performed in a laboratory-built, magnetically shielded furnace, with a residual field less than 10nT. Temperature increments of 20 °C were applied starting from room temperature and progressing up to a maximum temperature of 460 °C. Stepwise thermal demagnetization was applied to isolate the characteristic remanent magnetization (ChRM) and samples were measured on a 2G Entreprises DC Squid cryogenic magnetometer in a magnetically shielded room. Principal component analysis was used to calculate magnetic component directions from "Zijderveld" diagrams using Paleomagnetism.org (Koymans et al., 2020).

4.4. Cyclostratigraphy

The core 3AGN2S04 was tuned to the astronomical solution of Laskar et al. (2004) Northern Hemisphere (65°N) summer insolation, obliquity and eccentricity curves. The core has also been tuned to the Shackleton and Hall (1997) oxygen isotope record, obtained from site 926 and recovered during the Ocean Drilling Program (ODP) Leg 154 on the Ceara Rise, in the western equatorial Atlantic.

In this work, the cycles in the Tripoli Formation (1–49) refer to the numbering proposed by Hilgen and Krijgsman (1999) and Blanc-Valleron et al. (2002), whereas the lithological cycles of the CdB member refer to the one proposed by Caruso et al. (2015). In core 3AGN2S04, the classical triplet cycles made of marls, red laminites and diatomitic beds are not expressed. On the contrary, each cycle is made of gray silty clay alternating with dark laminated layers, and sometimes with whitish hard limestones. Key planktonic foraminifera events were found that permitted to accurately pinpoint the position of bio-events relative to the sedimentary cyclicity, using the eco-biostratigraphy proposed by Hilgen and Krijgsman (1999), Sierro et al. (2001), Blanc-Valleron et al. (2002) and Zachariasse et al. (2021). In the CdB member, bio-events are absent (because of harsh paleoenvironmental conditions) and the age model is entirely based on astronomical tuning of the lithological cycles expressed by organic-rich shale and carbonate alternations (Caruso et al., 2015). The organic-rich shales represent more humid periods during a higher sea level and have been correlated with insolation maxima, while the carbonate beds record drier periods during insolation minima with a lower sea level. The eccentricity curve has also been a useful tool to identify clusters of cycles, taking into

consideration that eccentricity has an influence on the lithological expression. During eccentricity minima lithological variations are less expressed and sedimentation of carbonates is less significant. Carbon stable isotope curves have also been used, correlating lighter values with eccentricity minima. Several key-sections located throughout the Caltanissetta Basin were chosen in order to carry out a detailed comparison, the outcrops of Marianopoli and Torrente Vaccarizzo, located in the northernmost and shallower part of the Caltanissetta Basin, and the outcrops of Serra Pirciata and Falconara/Gibliscemi located in the southernmost and deeper part of the Caltanissetta Basin. The Sorbas (Spain) and Metochia sections (Gavdos, Greece), respectively located in the western and the eastern Mediterranean basins, were also used for a more integrated correlation throughout the Mediterranean.

5. Results

5.1. Lithological description (110 to 60 m)

The Upper Gypsum unit (110 to 60 m) (Fig. 2) consists of i) gray laminated marls in which thin organic-rich layers are intercalated (from 110 to 105 m), ii) marls (from 105 to 93 m), iii) laminated brown/reddish to gray gypsarenites (from 93 to 85 m). From 85 to 65 m, the latter lithologies are repeated, with marls between 85 and 82.4 m and laminated brown to gray gypsarenites between 78.5 and 62.5 m. Sediment loss does not permit to describe the core from 82.4 to 78.50 m. From 62.5 to 60 m, gypsum is characterized by chicken-wire nodular structures.

5.2. Micropaleontological analysis

5.2.1. Foraminifera

In the Terravecchia Formation (270 to 220 m), the foraminiferal assemblages are poor and badly preserved, dispersed in a large quantity of quartz, feldspars, micas and pyrite grains typical of continental inputs. Among planktonic species, common individuals of *Globigerinoides obliquus obliquus*, *G. quadrilobatus*, *Globigerina bulloides*, *Neogloboquadrina acostaensis and N. humerosa* are present. In this interval, *Globorotalia menardii* and *G. suterae* have not been found. Rare specimens of *Globorotalia saphoe* (only 1–2 individuals) have been recognized at 243.8 m and 237.8 m. According to Sierro et al. (1993) and Zachariasse et al. (2021), this species belongs to the *G. miotumida/G. conomiozea* group and occurs with two influxes in the uppermost part of the MMi12a biozone (Fig. 3) (Lirer et al., 2019 and reference therein), predating the FO *G. suterae*. Planktonic foraminiferal samples from the Terravecchia Formation are also characterized by the presence of reworked species from lower Cretaceous (*Globigerinelloides* sp.) and lower Oligocene (*Pseudoastigerina micra*). Benthic foraminifera like *Elphidium*, *Ammonia*, *Nonion*, *Bolivina alata*, *Cassidulina carinata* and *Pandaglandulina dinapoli* are abundant and typical of shelf domain (Milker and Schmiedl, 2011; Caruso and Cosentino, 2014).

In the Tripoli Formation (220 to 182 m), the foraminiferal assemblage is richer in some particular layers, whilst in others foraminifera are rare or absent. The residual fraction is abundant in quartz, pyrite and carbonate grains especially in the uppermost part. Planktonic foraminifera are represented by only few species typical of the terminal part of Tripoli Formation (*Turborotalita multiloba*, *T. quinqueloba*, *N. acostaensis* in Fig. 4, *G. bulloides*, *G. obliquus obliquus*, *Globigerinella siphoniphera* and *Orbulina* spp.). In particular, five influxes of *T. multiloba* occur at 215.17 m, 212.24 m, 208.82 m, 204.93 m and 185.25 m (Fig. 3). The coiling direction of N. *acostaensis* changes throughout the core, with a dextral coiling direction from 213.38 to 207.78 m and a left dominant coiling from 205.88 to 204.93 m. Two peaks of *N. acostaensis* dextral coiling have also been recognized at 203.22 m and 185.25 m, and few specimens of *N. acostaensis* sinistral coiling at 185.25 m and 176.68 m. Species generally present elsewhere in the first 24 cycles of Tripoli Formation have not been found in the studied interval. The benthic foraminifera are dominated by *Bolivina* spp., *Bulimina elongata* and *Bulimina aculeata* (Fig. 4), typical species of stressed and hypoxic environments (Kouwenhoven et al., 2003; Kouwenhoven and van der Zwaan, 2006; Caruso et al., 2011).

In the CdB member (182 to 110 m), rare and badly preserved foraminifera considered as reworked have been found in the brecciated organic-rich shales intercalated between the carbonate beds. For this reason, the CdB member is assigned to the "Non Distinctive" zone (Fig. 3) (Lirer et al., 2019 and references therein).

In the Upper Gypsum unit (110 to 60 m), microfauna occurs in the gray clays. Brackish and marine fauna is observed at four levels, respectively at 83.5 m, 101 m, 103 m and at 107 m (Fig. 3). Rare specimens of *Haynesina* and *Cribroelphidium* have been found in layers where common valves of ostracods are present. They are the only foraminifera considered as autochthonous here, whilst rare shells of planktonic foraminifera of Paleogene age are badly preserved and therefore interpreted as reworked.

5.2.2. Calcareous nannoplankton

From the 26 analyzed samples of the interval between ~147 and ~ 245 cm (Fig. 2), 10 were totally barren, in particular samples between ~147 and ~ 204 cm. The calcareous nannofossil association is poorly preserved with evident signs of dissolution and/or recrystallization. Reworked taxa from Paleocene to middle Miocene are very abundant in all samples and rare Cretaceous reworked taxa are also present. Samples collected in the Terravecchia Formation between 231 and 245 m are characterized by a mélange of Oligocene to Miocene long-range taxa and cannot be attributed to a specific biozone. A reliable biostratigraphic attribution can be obtained only for samples collected at 207.75 and 218.91 m, respectively attributable to the lower Messinian (upper part of the MNN11c zone; *Sphenolithus abies*, small reticulofenestrids <3 μm) and to the upper Tortonian (MNN11a zone; *Discoaster pentaradiatus, D. brouweri*). Samples collected within the lithological interval referable to the Tripoli Formation at 198.44 and 199.91 m are entirely constituted by lower-middle Paleocene reworked taxa (*Fasciculites tympaniformis, Heliolithus kleinpellii*).

5.2.3. Ostracods

Rare disarticulated valves of adults and juveniles of the euryhaline and shallow-water *Cyprideis* sp. have been found in the gray marls of the Upper Gypsum unit between 103.50 and 106.48 m and 106.94 and 106.92 m. *Cyprideis* sp. becomes more abundant between 83.53 and 83.56 m, where both articulated (carapaces) and disarticulated valves belonging to different moult stages are observed, together with rare specimens of *Loxoconcha muelleri* (Fig. 4).

5.2.4. Other fossils

In the residual fraction >63 μm, radiolarians and pteropods have been randomly found. A 3 cm-thick layer rich in pteropods belonging to the *Creseis* genus has been observed in the Terravecchia Formation between 235.68 and 235.71 m, as well as rare mollusk shells of Cardids. In the Tripoli Formation, *Spumellaria* radiolarians (Fig. 4) are present only in some selected layers (196.81 m, 193.5, 183.24 m and 176.68 m). Pteropods belonging to *Creseis* spp. are present between 206.70 and 206.80 m, whilst *Limacina trochiformis* and *Limacina* cf *lesueurii* have been recognized in three layers at 213.38–213.34 m, 204.93–204.90 m and 181.22–181.19 m (Figs. 3 and 4). The systematic classification of the last two species was not so evident due to the absence of well-preserved shells, and in fact only internal models made of pyrite have been found. On the contrary, at 181.22–181.19 m, *L.* cf *lesueurii* specimens have a pseudomorphic calcitic shell. Further, siliceous spicules of sponges (203.22–203.20 m, 196.81–196.79 m) and rare aculeus of irregular echinoids are present (215.17–215.23 m; 185.25–185.23 m) (Figs. 3 and 4).

5.3. Magnetostratigraphy

Paleomagnetic measurements indicate that the NRM intensity of the samples show significant changes throughout the core. The normal

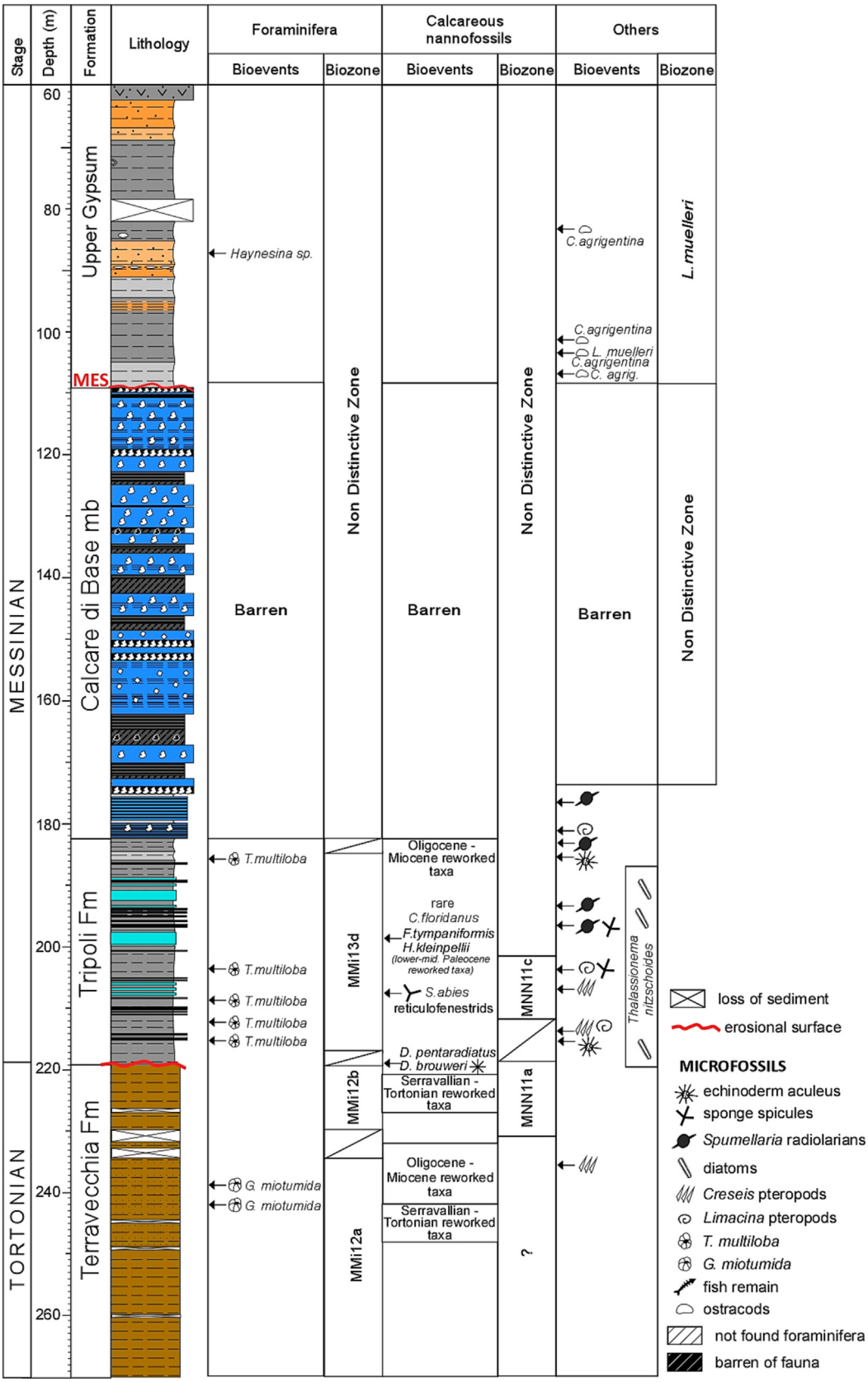

Fig. 3. Main microfauna - foraminifera, calcareous nannofossils and others - in core 3AGN2S04. MES is for "Messinian Erosional Surface".

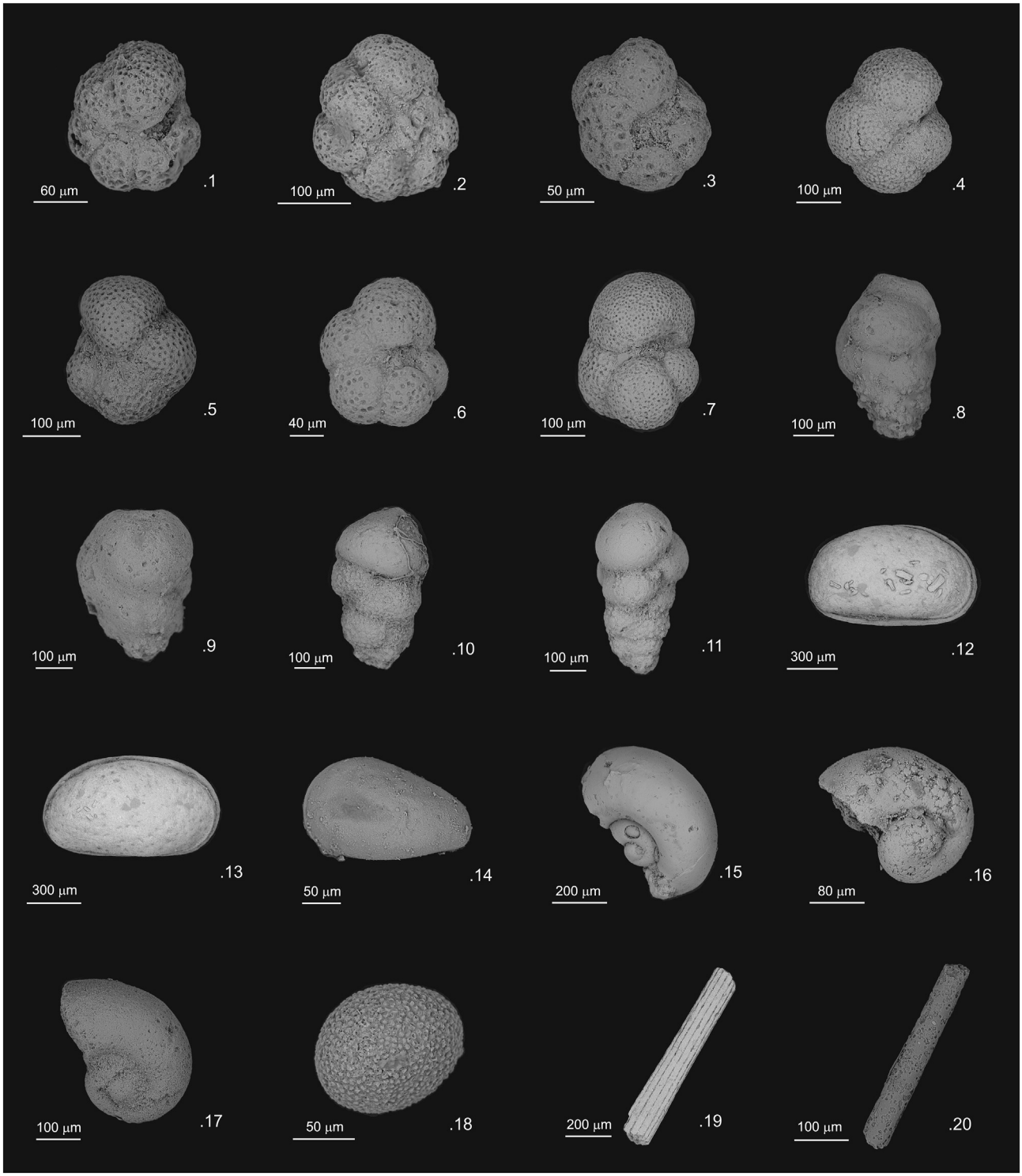

Fig. 4. 1) *Turborotalita multiloba* (umbilical side) – 212.24-212.22 m. 2) *Turborotalita multiloba* (spiral side) – 208.32-208.29 m. 3) *Turborotalita multiloba* (umbilical side) – 213.38-213.34 m. 4) *Neogloboquadrina acostaensis* left coiling (umbilical side) – 186.19-186.16 m. 5) *Neogloboquadrina acostaensis* right coiling (umbilical side) – 207.28-207.76 m. 6) *Turborotalita quinqueloba* (umbilical side) – 186.19-186.16 m. 7) *Globigerina bulloides* (umbilical side) – 186.19-186.16 m. 8) *Bulimina echinata* – 212.24-212.22 m. 9) *Bulimina echinata* – 212.24-212.22 m. 10) *Bulimina elongata* – 208.32-208.29 m. 11) *Bulimina elongata* – 208.32-208.29 m. 12) *Cyprideis agrigentina* (with 2 valves) – 104.40-104.38 m. 13) *Cyprideis agrigentina* (with 2 valves) – 104.40-104.38. 14) *Loxoconcha muelleri* – 104.40-104.38 m. 15) *Limacina* sp. pteropod – 208.32-208.29 m. 16) *Limacina* sp. pteropod with pyritized test – 208.32-208.29 m. 17) *Limacina* sp. pteropod – 208.32-208.29 m. 18) *Spumellaria* radiolarian – 208.32-208.29 m. 19) spine of irregular echinoid – 213.38-213.34 m. 20) sponge spicule – 196.81-186.79 m.

polarity samples of the upper part (S04–1-3, UG) and the base (S04–19, Terravecchia) are the strongest, ranging 200–2000 μA/m, and samples of especially the Tripoli Fm are very low, 1–100 μA/m. Samples of the Calcare di Base are all reversed revealing intensities between 11 and 400 μA/m. Thermal demagnetization curves generally reveal a single magnetic component of dual polarity that linearly decreases to the origin in the temperature range 100–300 °C. Some samples (S04–11,12) show two components, a reversed component in the 100–300 °C that

does not decay to the origin, and a second component of normal polarity. Heating the samples to temperatures above 350 °C generally results in erratic behavior and increased magnetization, which is most likely related to the transformation of pyrite into magnetite. Seven samples had too low intensity or showed only erratic behavior and could not be interpreted. Plotting the results in stratigraphic order show normal polarity at the base and top and a long reversed polarity interval in the middle part of the core. We interpret these reversed components as primary magnetic signal. However, given the difference in intensity between the normal and reversed polarity samples, we cannot exclude here that the normal polarities may comprise a secondary viscous magnetization; e.g. a magnetization caused by a present-day field overprint.

6. Discussion: from pre-MSC to Stage 3 of the MSC

6.1. Terravecchia Fm: Tortonian/Messinian stratigraphic gap

The Messinian GSSP has been defined at the base of cycle OA15 at the Oued Akrech section in Morocco and it coincides with the First Common Occurrence (FCO) of *Globorotalia miotumida*, astronomically dated at 7.246 Ma (Hilgen et al., 2000, 2012). In core 3AGN2S04, the two influxes of globorotalids belonging to *G. miotumida* gr. recognized in the Terravecchia Formation could be positioned either, i) in MMi12a biozone corresponding to *G. miotumida* gr. FO, or ii) at the base of MMi13a biozone corresponding to *G. miotumida* gr. FCO (e.g. Lirer et al., 2019). However, the absence of *G. suterae* in the interval below the two *G. miotumida* influxes suggests that this interval belongs to the uppermost part of MMi12a biozone (Table 1), as described at the Falconara/Gibliscemi (F/G) composite section (i.e. Sprovieri et al., 1996). Further, the thick-shelled and conical morphology of the *G. miotumida* suggests that they correspond to the invasion of globorotalids in the Mediterranean during late Tortonian (Krijgsman et al., 1995), preceding the T/M boundary and dated around 7.8 Ma. However, the absence of *G. menardii* forms, do not let us indicate a more precise age (Table 1). The absence of *G. menardii* suggest change to shallow bathymetry of the basin, the strong influx of freshwater from the northern Maghrebian chain and/or cyclical fluctuations of this species. At 218.91 m, the calcareous nannofossils *Discoaster pentaradiatus* and *D. brouweri* calcareous nannofossils were found, confirming a late Tortonian age (MNN11a zone).

A stratigraphic gap separates the Terravecchia and Tripoli formations, revealed by the absence of a large part of the planktonic foraminiferal MMi13 biozone (Table 1). Several microfossil bio-events marking the Tortonian - Messinian Transition and used as a tool for understanding the biotic response to the progressive environmental change related to the restriction of the Mediterranean-Atlantic gateway during the pre-MSC (Bulian et al., 2022b), have not been found in core 3AGN2S04. The nannofossil bio-events (i.e *Amaurolithus* spp. and *Reticulofenestra rotaria)* that approximate the Tortonian/Messinian boundary at Oued Akrech and the F/G sections are also missing. Regarding the foraminiferal bio-events, it lacks: i) the FO and LO of *G. nicolae* (6.83–6.72 Ma) – assigned to cycles 10 to 14 at F/G section, ii) *N. atlantica* (6.65–6.425 Ma) ascribed in cycle 16–20 at F/G section, iii) the Last Occurrence (LO) of *G. miotumida* at 6.52 Ma, assigned to cycle 24 at F/G section, iv) the First Common Occurrence (FCO) of *T. multiloba* at 6.42 Ma, ascribed to cycle 29 at F/G section, and iv) *N. acostaensis* sinistral/dextral coiling change at around 6.35 Ma, ascribed to in cycle 32 at F/G section (Table 1) (Hilgen and Krijgsman, 1999; Blanc-Valleron et al., 2002; Lirer et al., 2019). These planktonic foraminiferal bio-events have been useful in the cyclostratigraphic tuning comparing F/G section with Torrente Vaccarizzo, Marianopoli and Serra Pirciata sections in the Caltanissetta Basin (Caruso, 1999; Bellanca et al., 2001; Caruso et al., 2015), but also with Sorbas composite section (Spain; Sierro et al., 2001) and Pissouri section (Cyprus, Krijgsman et al., 2002; Morigi et al., 2007). However, in core 3AGN2S04, the lack of these foraminiferal bio-events indicates that the first 38 cycles, corresponding to around 800 kyr of the lower Tripoli Formation, are missing. The occurrence of five influxes of *T. multiloba* confirms that the Tripoli Formation part of the studied core corresponds to F/G cycles 39–46 (Zachariasse and Lourens, 2021). The hiatus recognized in core 3AGN2S04 has thus removed the entire T/M boundary interval (Fig. 5). This suggests that the Terravecchia/Tripoli formations contact results from tectonic deformation, probably related to the numerous thrust and backthrust affecting the study area (Fig. 1b).

Table 1
The table reports the bio-events in the pre-MSC and MSC. Comparison between the data obtained by various authors and our study. Bio-events present (✓) or absent (✗) in core 3AGN2S04.

Lithology	Biostratigraphy	Hilgen and Krijgsman (1999); Hilgen et al. (2000)	Sierro et al. (2001)	Bellanca et al. (2001)	Blanc-Valleron et al. (2002)	Lirer et al. (2019)	Our study
Formation (this study)	Bio-events	Age (Ma)	Age (Ma)	Age (Ma)	Age (Ma)	Age (Ma)	Presence/Absence
Top of Tripoli	Last influx of *T. multiloba*					6.07	✓
Tripoli	2th influx of *N. acostaensis* sin.	6.087	6.082			6.08	✓
Tripoli	5th *T. multiloba*		6.11			6.11	✓
Tripoli	*N. acostaensis* sin. influx (90 %)	6.126	6.126		6.13	6.12	✓
Tripoli	4th *T. multiloba*		6.16				✓
Tripoli	3th influx of *T. multiloba*		6.18				✓
Tripoli	2th influx of *T. multiloba*		6.23			6.23	✗
Tripoli	*G. scitula* group influx	6.295	6.291			6.29	✓
Tripoli	*N. acostaensis* S/D coiling change	6.337	6.360	6.35	6.34	6.35 MMi13d	✗
Tripoli	*T. multiloba* FCO	6.415	6.415	6.4	6.415	6.42	✗
Tripoli	*N. atlantica* LCO			6.43	6.425		✗
Tripoli	G. miotumida gr. LO	6.506	6.504	6.53	6.51	6.52	✗
Tripoli	*N. atlantica* FCO			6.64	6.65		✗
Tripoli	*G.nicolae* LO	6.722	6.713	6.73	6.72	6.72 MMi13c	✗
Tripoli	*G. nicolae* FO		6.828		6.82	6.83 MMi13b	✗
Terravecchia	*G. suterae* LO					7.16	✗
Terravecchia	*G. menardii* 5 LCO					7.23	✗
Terravecchia	*Globorotalia miotumida* FCO (Tortonian/Messinian boundary)	7.243	7.242		7.16	7.246	✓
Terravecchia	Influx of globorotalid conical forms *G. miotumida* gr.					7.89 MMi12a	✓

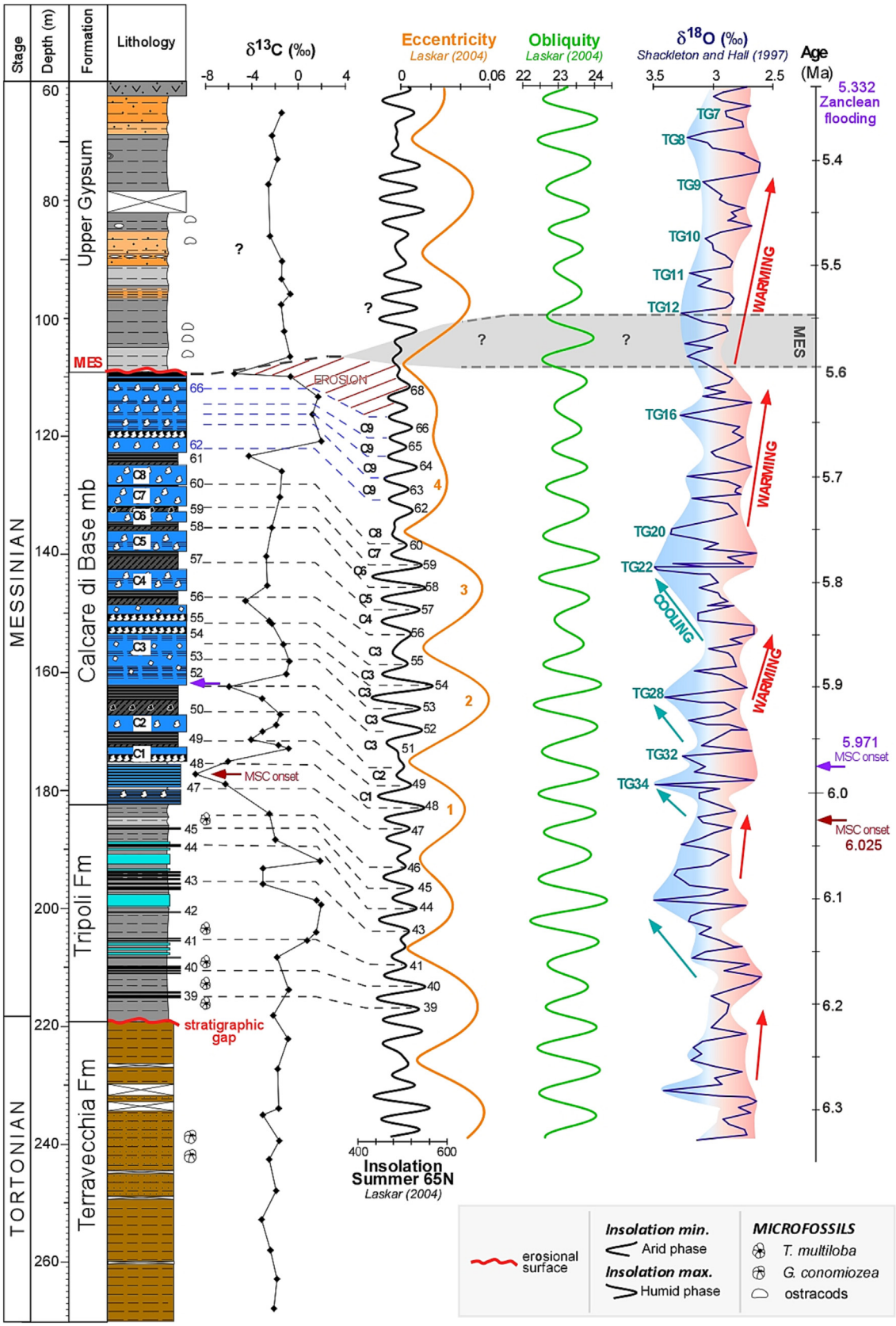

Fig. 5. Correlation of core 3AGN2S04 with astronomically-tuned (65°N summer insolation, eccentricity and obliquity curves; Laskar et al., 2004), carbon isotopes (from Tzevahirtzian et al., 2022) and benthic foraminifer oxygen isotopes (from Shackleton and Hall, 1997). Sapropels/shales are correlated to the insolation maxima, corresponding to humid phases, while carbonates are correlated to the insolation minima, corresponding to dry phases (Hilgen et al., 1995). black dotted line: calibration to shales; blue dotted line: calibration to carbonates; violet arrow: MSC onset (first gypsum) according to Roveri et al. (2014); red arrow: MSC onset proposed in this study (first calcare); MES is for "Messinian Erosional Surface".

6.2. The Tripoli Fm: calibration of the astronomical record

The scarce preservation and the rare presence of in situ calcareous nannoplankton and planktonic foraminifera does not permit astronomical tuning of the Terravecchia Formation. In the Tripoli Formation, key planktonic foraminifera accurately pinpoint the position of selected bio-events in lithological cycles. The five influxes of *T. multiloba* recognized in the studied core (Table 1) correspond to the uppermost part of Tripoli Formation as described at the Falconara section (Hilgen and Krijgsman, 1999; Blanc-Valleron et al., 2002) and at the Upper Abad marls of Sorbas (Spain; Sierro et al., 2001). Following the chronology proposed by Zachariasse and Lourens (2021), *T. multiloba* influxes are recognized in cycles 39, 40, 41, 42 and 46 of Falconara and in cycles UA23, UA24, UA25, UA26 and UA31 of Sorbas (Fig. 6). They fall into the MMi13d biozone sensu Lirer et al. (2019) and were astronomically dated, respectively from bottom to top, at 6.18 Ma, 6.16 Ma, 6.11 Ma and 6.07 Ma, covering two eccentricity cycles and eight precessional/insolation cycles. *N. acostaensis* dextral coiling is dominant from the base of Tripoli Formation, whilst the peaks of *N. acostaensis* sinistral coiling at 205.88 m and 203.22 m confirm cycles 42/43. The predominance of *N. acostaensis* dextral forms at 185.25 m falls between cycles 45/46, as described in Falconara (Blanc-Valleron et al., 2002). The calcareous nannoplankton assemblage of 3AGN2S04 is characterized by an oligotypic assemblage dominated by *Sphenolithus abies*. A similar association has also been described at Falconara section where the abundance of *Sphenolithus* gr. increases from cycle 33 of the Tripoli Formation and upwards (Blanc-Valleron et al., 2002) (Fig. 6), while in the Perales section (which is part of the Sorbas composite section) it starts from cycle UA24 of the Upper Abad member (Mancini et al., 2020). In the latter study, *S. abies* is followed or occurs together with *H. carteri*, *U. rotula* and *R. clavigera* calcareous nannoplankton species that directly predate the MSC onset. In our studied core, this assemblage has not been found, possibly due to bad preservation and the abundance of reworked Paleogene nannofossils. Moreover, at Falconara and Perales, *S. abies* coexist in the same interval with *T. multiloba* peaks (Blanc-Valleron et al., 2002; Mancini et al., 2020), hence the occurrence of both *S. abies* and *T. multiloba* in core 3AGN2S04 may be used as bio-events to confirm that this interval corresponds to the pre-MSC upper Tripoli Formation. The organic-rich dark layers of the Tripoli Formation have been considered as sapropels and correlated to the insolation maxima (Hilgen et al., 1995). Following the Falconara/Gibliscemi composite section (sensu Krijgsman et al., 1999a; Blanc-Valleron et al., 2002), the first sapropel of core 3AGN2S04 has been associated with the lithological cycle 39 (Figs. 5, 6). Consequently, the lithological cycle 42 is thinner and falls within an eccentricity minimum. The cluster of four lithological cycles 43–46 fits well with the eccentricity maximum.

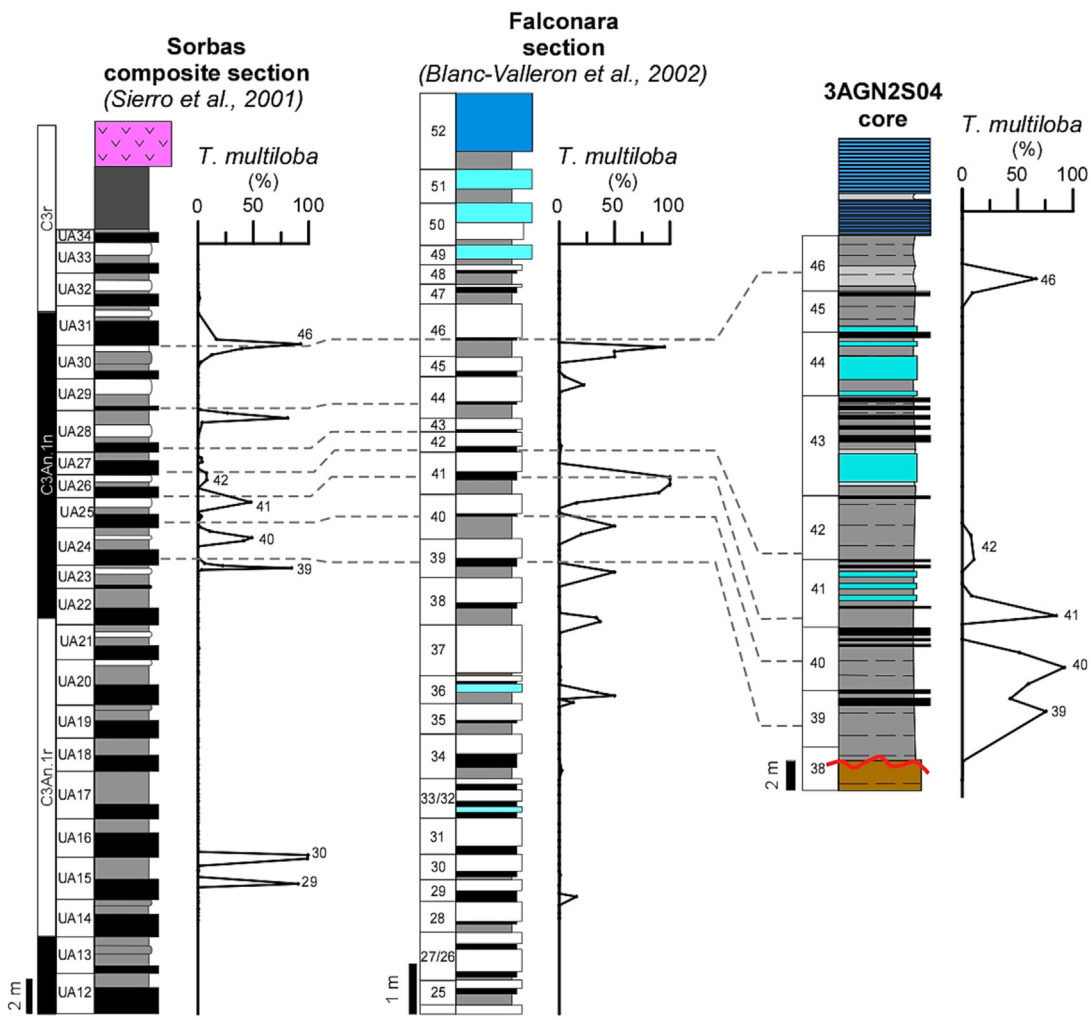

Fig. 6. Abundance variation of *Turborotalita multiloba* in different sections a) Sorbas (Spain), b) Falconara (southern Caltanissetta Basin, Sicily) compared to c) core 3AGN2S04 (northern Caltanissetta Basin, Sicily).

6.3. MSC Stage 1: the Calcare di Base

The transitional passage from the Tripoli Formation to the CdB member may be astronomically correlated with eccentricity maxima and the interval of maximal expression of insolation (Fig. 5). An age of around 6.00 and 6.05 Ma can be assigned to, respectively, the base of the first thick CdB carbonate bed C1 and the base of the underlying organic-rich shale interval. From the base of the CdB member (182 m), the $\delta^{13}C$ curve seems to fit with eccentricity periodicities, with lighter content correlated to the eccentricity minima, well revealed in cycle 50 (Fig. 5). The low $\delta^{13}C$ values measured within the thick organic rich shales are here considered equivalent to sapropels, showing events of extreme environmental change towards the establishment of eutrophic conditions (e.g. Tzevahirtzian et al., 2022). Above the dark black shales, the abundant presence of pseudomorphs of halite in microfacies in bed C1 testifies an evaporitic setting (e.g. Tzevahirtzian et al., 2022) and may be correlated with the lithological cycle 49 of Falconara/Gibliscemi Tripoli Formation. This tuning dates the beginning of the evaporitic conditions in our core at an astronomical age of 6.025 Ma ($\pm$ 3 kyr). Manzi et al. (2013) correlated the base of the Primary Lower Gypsum in Monte Tondo section (N. Italy) with the astronomical cycles and obtained an age of 5.969 Ma and 5.974 Ma, defining the MSC onset at 5.971 Ma, amending the previous date of 5.96 $\pm$ 0.02 Ma proposed by Krijgsman et al. (1999a, 1999b, 1999c). Hence, the MSC onset age that we propose in this study for core 3AGN2S04 is 50–60 ka earlier than the major onset proposed by Manzi et al. (2013) and by Krijgsman et al. (1999a, 1999b, 1999c), which implies that the onset of the CdB in the Caltanissetta Basin is earlier than the first gypsum bed in the other Mediterranean sections as already discussed by Rouchy and Caruso (2006) and Caruso et al. (2015). Unfortunately, the first gypsum bed in the Caltanissetta Basin has so far never been astronomically dated, so we cannot properly evaluate the local depositional delay between gypsum and limestone formation. At Santa Elisabetta and Ciminna, the MSC onset is marked by a gypsum bed that overlies clays rich in *T. multiloba* (Lo Cicero et al., 1997; Caruso et al., 2015); however, it has not been possible to astronomically date these gypsum beds.

In the CdB member, the cyclostratigraphic calibration is not as straightforward as for the pre-evaporites due to the absence of bio- and magnetostratigraphic constraints (Manzi et al., 2013; Caruso et al., 2015). Our 3AGN2S04 age model is entirely based on the astronomical tuning of the lithological cycles expressed by organic-rich shale and carbonate alternations. Four cycles of eccentricity maxima (Fig. 5) permitted to identify clusters in which the CdB carbonates have been grouped. Intervals of insolation/eccentricity maxima correlated to obliquity minima correspond to cooling periods culminating with glacial events (Shackleton and Hall, 1997). These clusters have also been defined in the $\delta^{13}C$ proxy, tuning the eccentricity minima to the lowest $\delta^{13}C$ values. Carbonate beds C1 and C2, together with the organic-rich shales, may be regarded as a cluster (1) and may be associated to precession minima between 48 and 49 and 49–50, respectively (Fig. 5). This interval corresponds to a small cooling period that culminates with the glacial event TG34. Therefore, carbonate beds C3 may be associated with cycles 51 to 55 that cover a whole 100 kyr eccentricity cycle (2) (Fig. 5). This interval also corresponds to strong climate oscillations characterized by the glacial event TG28 occurring when obliquity is reversed to eccentricity and insolation minima. The opposite trend between eccentricity and obliquity produces a less marked lithological cycle (53). Carbonate beds C4 to C8 may be regarded as cluster 3 in Fig. 5 and may correspond to cycles 56 to 60. This interval also corresponds to a progressive cooling period culminating with TG22 and TG20. Finally, carbonate bed C9 may contain several lithological cycles, where shales are not expressed, and corresponds to cycles 62 to 66. In this interval (4), the expression of insolation and eccentricity is less significant which may explain steadier conditions. Finally, the four eccentricity cycles tuned to the CdB member may consequently represent around 400 kyr, in good agreement with the total duration of ~380 ka of Stage 1 that resulted in an age of ~5.59 Ma for the top of the Primary Lower Gypsum (Roveri et al., 2014). During the CdB member interval, high annual rainfall during Northern Hemisphere summer insolation maxima (precession minima) results in higher freshwater discharge to the northern Caltanissetta Basin that generates stratification in the water body, warmer sea surface waters and reduced vertical mixing. These environmental conditions did permit the deposition of the laminated organic-rich shales but did not allow foraminifera or microalgae organisms to flourish due to the highly acidic water conditions (Tzevahirtzian et al., 2022). However, the enhanced river discharge results in higher siliciclastic particles to the northern Caltanissetta Basin increasing its relative concentrations in the sediments at the expense of the carbonate sediments. During Northern Hemisphere summer insolation minima, conditions are drier and saltier and a lower river discharge to the northern Caltanissetta Basin induces evaporation. A shallower and mixed water body is then established that permits the formation of carbonates.

6.4. Stage 2: the MES

Cycle 66 marks the uppermost CdB while the passage from the CdB member to the Upper Gypsum (UG) unit may be correlated with the not well-expressed Northern Hemisphere summer insolation and the eccentricity minima (Fig. 5) that corresponds to the main desiccation phase of the Mediterranean (MES). The missing cycles 67 and 68 may have not been deposited or may have been eroded during the desiccation event (Fig. 5). Moreover, in the UG unit, 7 to 8 sedimentary cycles were described throughout the Mediterranean (Vai, 1997; Krijgsman et al., 2001; Fortuin and Krijgsman, 2003). In core 3AGN2S04, only the lowermost UG unit has been recovered and correlations with the astronomical curves remain inconclusive. The onset of the UG unit follows the main desiccation phase of the Mediterranean (MES) (Ryan, 2009) and may be associated with the eustatic sea level rise and a progressively warming climate.

6.5. MSC stage 3: the Upper Gypsum

A drastic change of lithology between the CdB member and the UG unit, characterized by a black colored sediment layer (F in Fig. 2) similar to a paleosol, that progressively becomes brecciated may record a phase of continental exposure after the desiccation. At Pissouri in Cyprus, a paleosol has been associated with the MES (Rouchy, 1982). This paleosol is similar with the black interval observed between the CdB member and the Upper Gypsum unit in 3AGN2S04, and may correspond to the MES as well. However, further investigation needs to be done.

In the upper part of core 3AGN2S04, the lowermost interval of the UG is constituted by gray marls, laminar gypsarenites and nodular gypsum (Fig. 2). In some gray marl layers, poorly diversified microfaunal assemblages (benthic foraminifera and ostracods) occur. *Cyprideis* sp. is the most common and abundant among the recognized microfossils. Living relatives of this genus, *C. torosa*, do not provide salinity information, because of their euryhaline distribution, but *Cyprideis* is a good water depth indicator, as it tolerates only a few tens of meters of water (Neale, 1988; Meisch, 2000; Meyer et al., 2016). Rare specimens of *Loxoconcha muelleri* are also found together with *Cyprideis* sp. in one sample 83.53–83.56 m. Although *L. muelleri* does not have living relatives that can provide us with paleoecological information, studies of sedimentary records in the Eastern and Central Paratethys, where this taxon is first described, suggest that it also inhabited shallow environments, possibly at salinities in the range of the low mesohaline field (Rausch et al., 2021 and references therein). In these layers, rare euryhaline benthic foraminifera like *Haynesina* and *Cribroelphidium,* typical of shallow water and able to survive in low mesohaline conditions, were found. Altogether, the microfossil content of the UG unit suggests that it deposited in shallow-water habitats possibly featured by low mesohaline conditions, although the establishment, at times, of both

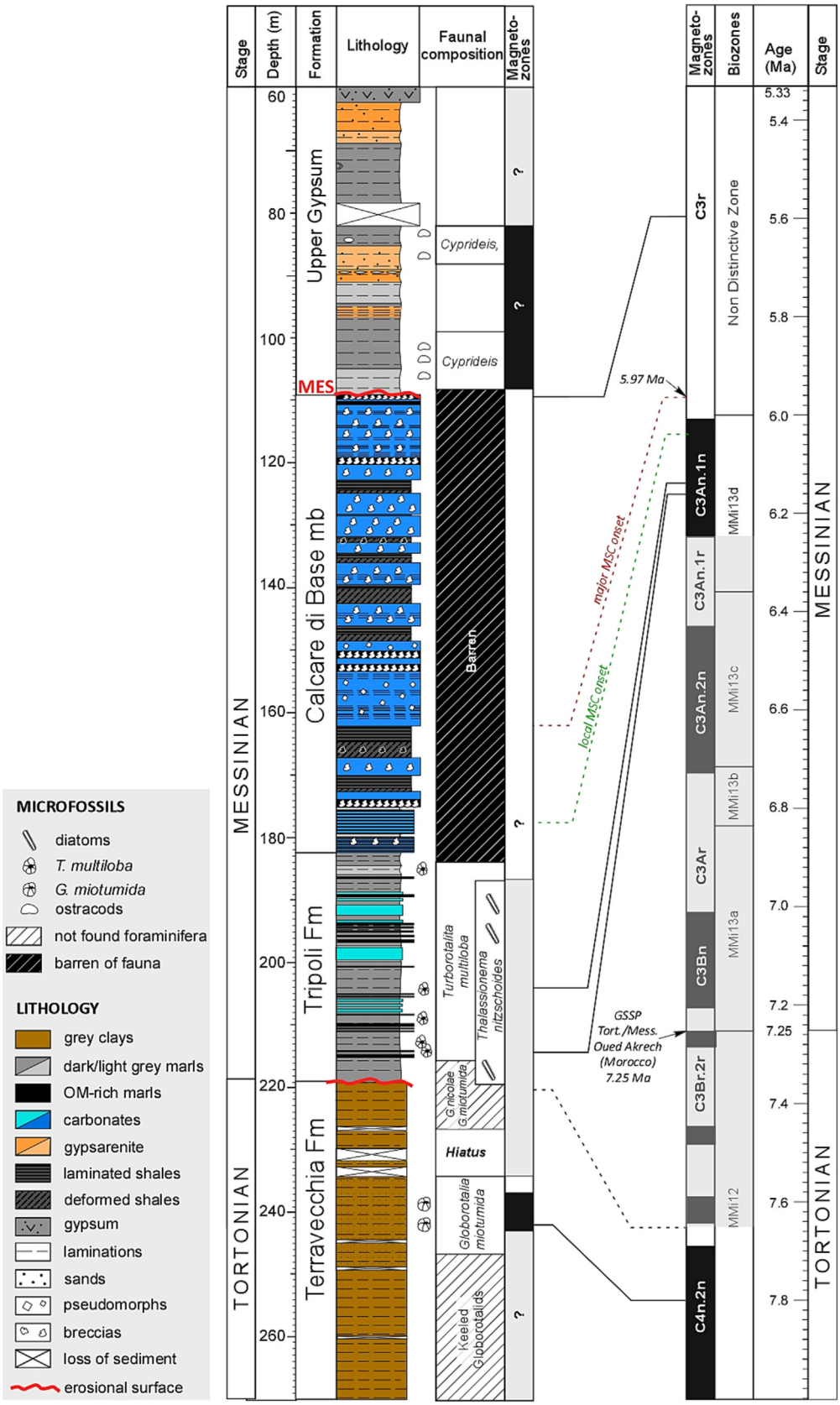

Fig. 7. Biostratigraphy and magnetostratigraphy of core 3AGN2S04.

lower and higher salinity conditions cannot be ruled out. The nodular gypsum characterized by chicken-wire structures observed at the top may results from the rehydration of anhydrite that formed by early diagenetic growth. Rouchy et al. (1998) have observed some beds of nodular gypsum in the Lorca Basin (SE Spain) and argue that they were deposited during periods of subaerial exposure (sabkha conditions).

6.6. Integrated stratigraphic framework for the MSC successions of the Caltanissetta Basin

Our magnetostratigraphic analyses allowed the identification of two short normal and one relatively long reversed polarity interval. The lowermost normal interval corresponds to the Terravecchia Fm. Two *G. miotumida* group influxes occur in this normal polarity interval, in accordance with what is described by Krijgsman et al. (1995) at the Gibliscemi and Faneromeni sections, where the two influxes fall into the magnetic subchron C4n2n. Thus, the uppermost part of Terravecchia Formation corresponds to subchron C4n.1r, which provides an age range of 7.642–7.695 Ma (Fig. 7). According to Hilgen et al. (2000), the Tortonian/Messinian boundary falls within the brief reserved subchron C3Br.1r coinciding with the *G. miotumida* FCO. Their sections on Crete are the only cyclically-bedded units in the Mediterranean that provide a reliable magnetostratigraphy for this interval (Krijgsman et al., 1994; Krijgsman et al., 1995), while the Abad sections of Spain (Sierro et al., 2001) and the Falconara/Gibliscemi (F/G) composite section in the Caltanissetta Basin are the only ones that have been correlated on a bed-to-bed scale (Hilgen et al., 1995; Krijgsman et al., 1995). Magnetostratigraphic correlations date the base of Tripoli of F/G section between C3Bn and the lowermost part of C3R (Krijgsman et al., 1999a), whilst the Upper Abad Formation spans from C3Ar to C3r (pars) (Sierro et al., 2001). The magnetic signal in the corresponding interval of our core unfortunately did not provide any reliable results. At Sorbas, the last five influxes of *T. multiloba* fall into C3An.1n. Thanks to the bio-events recognized in our studied core, the five influxes of *T. multiloba* occur in the MMi13d biozone and may be correlated with subchron C3An.1n (Fig. 3.6). Finally, we conclude that the interval of the Tortonian – Messinian Transition (up to 6.25 Ma) is not present and in consequence five normal and five reversal chrons (subchrons) are missing (Fig. 7). The entire Calcare di Base succession at 3AGN2S04 only shows reversed polarity samples, in good agreement with the general correlation to chron C3r. The Upper Gypsum unit falls within the magnetic reversal chron C3r as well (Van der Laan et al., 2006; Hilgen et al., 2007). The samples of the assumed UG formation in our core are, however, all of normal polarity. This results in two different explanations: 1) the normal signal is an overprint of the present-day magnetic field or 2) the upper part of the core does not correspond to the UG but corresponds in fact to the younger Zanclean Thvera subchron (C3r.4n). We consider option 1 as the most likely here.

A few reliable biostratigraphic events were recognized in core 3AGN2S04 that permitted to confirm the dated Mediterranean planktonic foraminiferal biostratigraphic zonation of the late Tortonian and Messinian MSC onset (Hilgen and Krijgsman, 1999; Hüsing et al., 2009; Krijgsman et al., 1999a, 1999b, 1999c; Sierro et al., 2001). The integrated biostratigraphic analysis allowed a bed-to-bed correlation of core 3AGN2S04 with the reference composite sections of Falconara/Gibliscemi (F/G; Sicily) and Sorbas (Spain), as well with various other sections from the Caltanissetta Basin (Fig. 8). The cyclostratigraphic correlation between the F/G section with those of Torrente Vaccarizzo, Marianopoli and Serra Pirciata have already been discussed (Caruso, 1999; Bellanca et al., 2001; Sierro et al., 2001; Caruso et al., 2015) and

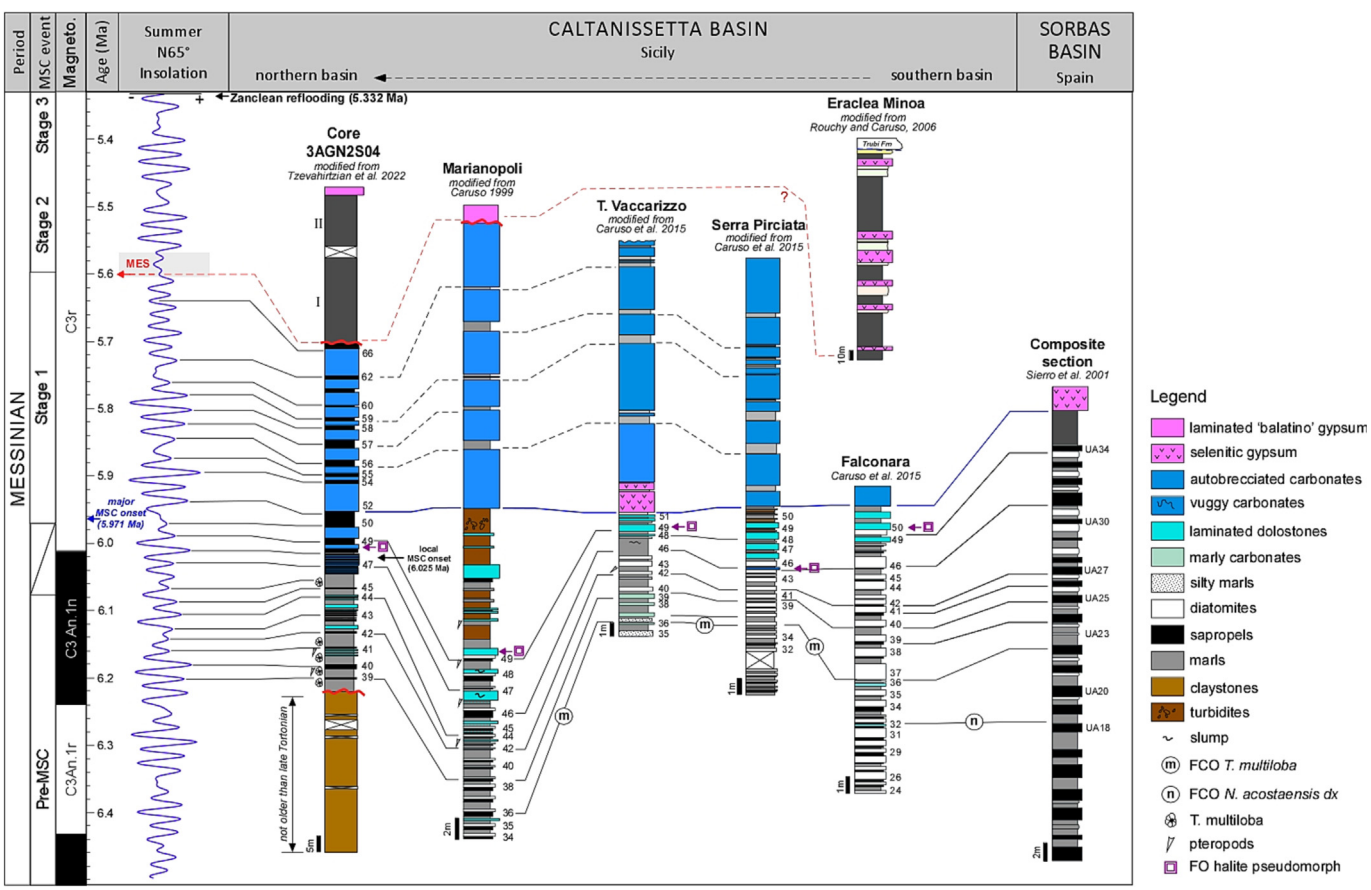

Fig. 8. Bio-cyclostratigraphic correlation of core 3AGN2S04 with Marianopoli (modified from Caruso, 1999), Torrente Vaccarizzo, Serra Pirciata, Falconara (modified from Caruso et al., 2015) and Eraclea Minoa (modified from Rouchy and Caruso, 2006) sections from Caltanissetta Basin (Sicily) and with the reference composite section (from Sierro et al., 2001) from Sorbas Basin (Spain). In the Tripoli Formation, core 3AGN2S04 lacks the first 38 cycles, more cycles than in the southern Caltanissetta. *T. multiloba* is present in the first lithological cycle of Tripoli Fm correlated with cycle 39 of Falconara. The blue arrow indicates the 'major MSC onset' at 5.971 Ma proposed by Manzi et al. (2013). In core 3AGN2S04, we propose a local MSC onset at 6.025 Ma, earlier than in other areas.

was supported by the FCO *T. multiloba* in cycle 36, located four lithological cycles above the *N. acostaensis* coiling change (cycle 32, 6.36 Ma), and astronomically dated at around 6.29 Ma. Five peaks of *T. multiloba* have been recognized in the uppermost part of Tripoli Fm at cycles 39, 40, 41, 42 and 46 (i.e. Blanc-Valleron et al., 2002) as well as at cycles U23, U24, U25, U28 and U30 from Sorbas section (i.e. Sierro et al., 2001).

The rhythmic deposition of the CdB carbonates and organic-rich shales in core 3AGN2S04 at the transition Tripoli/CdB were also observed at Gibliscemi, Serra Pirciata, Torrente Vaccarizzo (Caruso et al., 2015) and Marianopoli (Birgel et al., 2014) sections in the Caltanissetta Basin. We consider these lithological cycles precessionally controlled. However, the sedimentological response to the climate fluctuations may vary from one sub-basins to another and depends on local paleobathymetry. In fact, the variable lithological cycles and presence/absence of bio-events throughout the Caltanissetta Basin seems to be dependent on the local history of every basin. The first appearance of the CdB facies containing halite pseudomorphs reflects the onset of evaporite deposition triggered by sea-level fluctuations. According to Rouchy and Caruso (2006), a cooling period at 6.26 Ma (Vidal et al., 2002; Shackleton and Hall, 1997) might have produced isochronous paleo-oceanographic events affecting the Mediterranean by triggering restricted conditions in marginal sub-basins, whereas in the deepest part the sedimentation was still marine, as for instance at Falconara. In core 3AGN2S04, we have assigned a local onset of the CdB at 6.025 Ma (± 3 kyr), 54 kyr earlier than the major MSC onset proposed by Roveri et al. (2014), 25 kyr later than the MSC onset proposed in Falconara (~6 Ma) by Zachariasse and Lourens (2021), and 5 to 115 kyr later than in most of other marginal areas of the Caltanissetta Basin, in which Rouchy and Caruso (2006) suggest that the first evidences of evaporitic conditions occurred around 6.03 Ma at Falconara-Gibliscemi, 6.06 Ma at Pietraperzia, 6.08 Ma at Serra Pirciata, 6.14 Ma at Monte Gallitano. This infer that the MSC/CdB onset occurred diachronously between sub-basins of Sicily, testified by the deposition of halite pseudomorphs in different beds of the CdB. For this reason, we introduce the term "local onset" in each sub-basin (Fig. 8). Caruso et al. (2015) already discussed that the transition between the Tripoli Formation and the CdB member is not a synchronous event within the Caltanissetta Basin, which means that the passage from marine conditions to restricted/hypersaline conditions was diachronous between the various Sicilian sub-basins. It is important to note that even if the climatic and paleo-oceanographic changes were isochronous events the sedimentary response was different.

7. Conclusion

The late Miocene deposits from core 3AGN2S04 document a key interval from pre-evaporitic sediments to the lower part of Upper Gypsum. Key bio-events and magnetic sub-chrons C4n.2n and C3An.1n were recognized in the pre-MSC Terravecchia and Tripoli formations and confirm the presence of a tectonic gap. The correlation of *T. multiloba* peaks to the reference sections of Falconara/Gibliscemi (Sicily) and Sorbas (Spain) allowed to identify the uppermost part of the Tripoli Formation, belonging to MMi13d pars. The first 38 cycles of the Tripoli Formation are missing in core 3AGN2S04. The barren sediments of the CdB member were defined as the 'Non Distinctive zone'. This lithology shows a cyclical pattern made of black shales alternated to brecciated/autobrecciated carbonates rich in halite pseudomorphs. On top of the CdB member (Stage 1 of the MSC), an unconformity with continental sediments has been recognized, here considered as equivalent of the Messinian Erosional Surface (MES, Stage 2). On top of the MES lies a 50 m-thick succession that we tentatively attribute to the Upper Gypsum Unit. A few marl samples contain low diversity assemblages of ostracods (*Cyprideis* sp. and *L. muelleri*) and foraminifera (*Haynesina* and *Cribroelphidium*) that indicate deposition in shallow-water (<30 m) and possibly low mesohaline habitats. The integrated bio-cyclostratigraphic analysis allowed a bed-to-bed correlation of the studied core with Falconara/Gibliscemi and Sorbas and with various other sections from the Caltanissetta Basin. Lithological cyclicities have been calibrated to the astronomical solution of Laskar and seem to be controlled by Milankovitch periodicities. The first evaporitic carbonate in core 3AGN2S04, dated here at an astronomical age of 6.025 Ma (± 3 kyr), occurs 3 precessional cycles before the first gypsum bed of the classical MSC sections, which is dated at 5.971 Ma (Manzi et al., 2013). The diachronous onset of evaporitic conditions depends on the regional position of the outcrops in the Sicilian sub-basins and is related to the local paleoenvironmental conditions during the deformation of the front of Maghrebian chain, inferring that the establishment of hypersaline and restricted conditions throughout the Caltanissetta basins occurred diachronously.

Data availability

Data will be made available on request.

Declaration of competing interest

The authors declare that they have no known competing financial interests or personal relationships that could have appeared to influence the work reported in this paper.

Acknowledgments

This research was supported by the project SALTGIANT-Understanding the Mediterranean Salt Giant which funding was provided by the European Union's Horizon 2020 research and innovation programme under the Marie Sklodowska-Curie grant agreement No 765256. We would like to thank all members of SALGIANT community for the inspiring discussions during workshops, training courses and fieldtrips. We acknowledge the geologist Paolo Vizzi and the geologist and technical director of the GEO GAV Srl Company, Giuseppe Alba, for inviting us on the field during the drilling of core 3AGN2S04, as well as the Italian Railway State Company Italferr for providing us with this fresh core after the geotechnical analysis undertaken in the construction project of the Palermo-Catania railway in Sicily. We also thank the Master student Giuseppe Messina that helped us to carry the numerous core boxes, to store them to DISTeM (UNIPA) and to do a detailed sampling of the core. We also thank Francesco Bonomo for the technical support during SEM acquisition at the ATEN (Advanced Technologies Network) Center of the University of Palermo. Finally, we greatly thank the editor Catherine Chagué, the reviewer Jesus M. Soria and two anonymous reviewers for the fruitful comments provided, that led to the improvement of the manuscript.

References

Andreetto, F., Aloisi, G., Raad, F., Heida, H., Flecker, R., Agiadi, K., Lofi, J., Blondel, S., Bulian, F., Camerlenghi, A., Caruso, A., Ebner, R., Garcia-Castellanos, D., Gaullier, V., Guibourdenche, L., Gvirtzman, Z., Hoyle, T.M., Meijer, P.T., Moneron, J., Sierro, F.J., Travan, G., Tzevahirtzian, A., Vasiliev, I., Krijgsman, W., 2021. Freshening of the Mediterranean Salt Giant: controversies and certainties around the terminal (Upper Gypsum and Lago-Mare) phases of the Messinian Salinity Crisis. Earth Science Reviews 216, 103577. https://doi.org/10.1016/j.earscirev.2021.103577.

Andreetto, F., Flecker, R., Aloisi, G., Mancini, A.M., Guibourdenche, L., de Villiers, S., Krijgsman, W., 2022. High-amplitude water-level fluctuations at the end of the Mediterranean Messinian Salinity Crisis: implications for gypsum formation, connectivity and global climate. Earth and Planetary Science Letters 595. https://doi.org/10.1016/j.epsl.2022.117767.

Bellanca, A., Caruso, A., Ferruzza, G., Neri, R., Rouchy, J.M., Sprovieri, M., Blanc-Valleron, M.M., 2001. Transition from marine to hypersaline conditions in the Messinian Tripoli Formation from the marginal areas of the central Sicilian Basin. Sedimentary Geology 140, 87–105.

Bello, M., Franchino, A., Merlini, S., 2000. Structural model of Eastern Sicily. Memorie della Societa Geologica Italiana 55, 61–70.

Bianchi, F., Carbone, S., Grasso, M., Invernizzi, G., Lentini, F., Longaretti, G., Merlini, S., Mostardini, F., 1987. Sicilia orientale: profilo geologico Nebrodi-Iblei. Memorie della Societa Geologica Italiana 38, 429–458.

Birgel, D., Guido, A., Liu, X.-L., Hinrichs, K.U., Gier, S., Peckmann, J., 2014. Hypersaline conditions during deposition of the Calcare di Base revealed from archaeal di- and tetraether inventories. Org. Geochem. 77. https://doi.org/10.1016/j.orggeochem.2014.09.002.

Blanc-Valleron, M.-M., Pierre, C., Caulet, J.P., Caruso, A., Rouchy, J.M., Cespuglio, G., Sprovieri, R., Pestrea, S., Di Stefano, E., 2002. Sedimentary, stable isotope and micropaleontological records of paleoceanographic change in the Messinian Tripoli Formation (Sicily, Italy). Palaeogeography, Palaeoclimatology, Palaeoecology 185, 255–286.

Borrelli, M., Perri, E., Critelli, S., Gindre-Chanu, L., 2020. The onset of the Messinian Salinity Crisis in the central Mediterranean recorded by pre-salt carbonate/evaporite deposition. Sedimentology 68. https://doi.org/10.1111/sed.12824.

Bown, P.R., Lees, J.A., Young, J.R., 2004. Calcareous nannoplankton evolution and diversity through time. In: Thierstein, H.R., Young, J.R. (Eds.), Coccolithophores. Springer, Berlin, Heidelberg https://doi.org/10.1007/978-3-662-06278-4_18.

Bulian, F., Kouwenhoven, T.J., Andersen, N., Krijgsman, W., Sierro, F.J., 2022a. Reflooding and repopulation of the Mediterranean Sea after the Messinian Salinity Crisis: benthic foraminifera assemblages and stable isotopes of Spanish basins. Mar. Micropal. 176. https://doi.org/10.1016/j.marmicro.2022.102160.

Bulian, F., Kouwenhoven, T.J., Jiménez-Espejo, F.J., Krijgsman, W., Andersen, N., Sierro, F.J., 2022b. Impact of the Mediterranean-Atlantic connectivity and the late Miocene carbon shift on deep-sea communities in the Western Alboran Basin. Palaeogeography, Palaeoclimatology, Palaeoecology 589. https://doi.org/10.1016/j.palaeo.2022.110841.

Butler, R.W.H., Lickorish, W.H., Grasso, M., Pedley, H.M., Ramberti, L., 1995. Tectonics and sequence stratigraphy in Messinian basins, Sicily: constraints on the initiation and termination of the Mediterranean salinity crisis. Geological Society of America Bulletin 107, 425–439.

Caruso, A., 1999. Biostratigrafia, Ciclostratigrafia e Sedimentologia dei Sedimenti Tripolacei e Terrigeni del Messiniano Inferiore, Affioranti nel Bacino di Caltanissetta (Sicilia) e nel Bacino di Lorca (Spagna). (Ph. D. Thesis)Palermo-Napoli University (232 pp.).

Caruso, A., Cosentino, C., 2014. Classification and taxonomy of modern benthic shelf foraminifera of the central Mediterranean sea. In: Dan Georgescu, M. (Ed.), Foraminifera. Nova Publishers, pp. 249–313.

Caruso, A., Cosentino, C., Tranchina, L., Brai, M., 2011. Response of benthic foraminifera to heavy metal contamination in marine sediments (Sicilian coasts, Mediterranean Sea). Chemistry and Ecology 27, 9–30.

Caruso, A., Pierre, C., Blanc-Valleron, M.-M., Rouchy, J.M., 2015. Carbonate deposition and diagenesis in evaporitic environments: the evaporative and sulphur bearing limestones during the settlement of the Messinian salinity crisis in Sicily and Calabria. Palaeogeography, Palaeoclimatology, Palaeoecology 429, 136–162.

Catalano, R., 1979. Scogliere Ed Evaporiti Messiniane In Sicilia. Modelli Genetici Ed Implicazioni Strutturali. Lavori Istituto Di Geologia Di Palermo N° 18.

Catalano, R., Franchino, A., Merlini, S., Sulli, A., 2000. Central Western Sicily structural setting interpreted from seismic reflection profiles. Memorie della Societa Geologica Italiana 55, 5–16.

Catalano, R., Valenti, V., Albanese, C., Accaino, F., Sulli, A., Tinivella, U., Gasparo Morticelli, M., Zanolla, C., Giustiniani, M., 2013. Sicily's foldthrust belt and slab roll-back: the SI.RI.PRO. Seismic crustal transect. Journal of the Geological Society, London 170, 451–464.

Cita, M.B., Colombo, L., 1979. Sedimentation in the latest Messinian at Capo Rossello (Sicily). Sedimentology 26, 497–522.

Cita, M.B., Ryan, W.B.F., 1978. Messinian erosional surfaces in the Mediterranean. Marine Geology 27 (3–4), 193–395.

Decima, A., Wezel, F.C., 1971. Osservazioni sulle evaporiti Messiniane della Sicilia centromeridionale. Rivista Mineraria Siciliana 130–134, 172–187.

Decima, A., Wezel, F.C., 1973. Late Miocene evaporites of the central Sicilian basin, Italy. In: Ryan, W.B.F., Hsü, K.J., et al. (Eds.), Initial Reports of the Deep Sea Drilling Projecvol. 13. U.S.Govt. Printing Office, Washington, pp. 1234–1240.

Decima, A., McKenzie, J., Schreiber, B.C., 1988. The origin of evaporative carbonates. Journal of Sedimentary Petrology 58, 256–272.

Di Grande, A., Giandinoto, V., 2002. Plio-Pleistocene Sedimentary Facies and their Evolution in Centre-South-Eastern Sicily: a Working Hypothesis. Stephan Mueller Special Publication Series 1, 211–221.

Doglioni, C., 1990. The global tectonic pattern. Journal of Geodynamics 12 (1), 21–38.

Facenna, C., Becker, T.W., Lucente, F.P., Jolivet, L., Rossetti, F., 2001. History of subduction and back-arc extension in the Central Mediterranean. Geophysical Journal International 145, 809–820.

Fortuin, A.R., Krijgsman, W., 2003. The Messinian of the Nijar Basin (SE Spain): sedimentation, depositional environments and paleogeographic evolution. Sedimentary Geology 160, 213–242.

Garcia-Veigas, J., Ortı, F.J., Rosell, L., Ayora, C., Rouchy, J.M., Lugli, S., 1995. The Messinian salt of the Mediterranean: geochemical study of the salt from the central Sicily basin and comparison with the Lorca Basin (Spain). Bulletin de la Société Géologique de France 166, 699–710.

Gautier, F., Clauzon, J.-P., Cravatte, J., Violanti, D., 1994. Age et durée de la crise de salinité messinienne. Comptes rendus de l'Académie des Sciences de Paris, t.318, série II 1103–1109.

Gindre-Chanu, L., Borrelli, M., Caruso, A., Critelli, S., Perri, E., 2020. Carbonate/evaporitic sedimentation during the Messinian salinity crisis in active accretionary wedge basins of the northern Calabria, southern Italy. Marine and Petroleum Geology 112. https://doi.org/10.1016/j.marpetgeo.2019.104066.

Grasso, M., Pedley, H.M., 1988. The sedimentology and development of Terravecchia Formation carbonates (Upper Miocene) of North Central Sicily: possible eustatic influence on facies development. Sedimentary Geology 57, 131–149.

Grasso, M., Pedley, H.M., 1989. Palaeoenvironment of the upper Miocene coral build-ups along the northern margins of the Caltanissetta Basin (central Sicily). Proc. 3rd Symp. Ecology and Palaeontology of Benthic Communities (Ed. DiGeronemo), Catania-Taormina, Oct. 12-16, 1985, Catania, pp. 373–389.

Grossi, F., Gliozzi, E., Anadon, P., Castorina, F., Voltaggio, M., 2015. Is Cyprideis agrigentina Decima a good paleosalinometer for the Messinian Salinity Crisis? Morphometrical and geochemical analyses from the Eraclea Minoa section (Sicily). Palaeogeography, Palaeoclimatology, Palaeoecology 419, 75–89.

Gugliotta, C., 2012. Inner vs. outer wedge-top depozone "sequences" in the late Miocene (late Tortonian-early Messinian) Sicilian foreland basin system; new data from the Terravecchia Formation of NW Sicily. Journal of Geodynamics 55, 41–55.

Hilgen, F.J., Krijgsman, W., 1999. Cyclostratigraphy and astrochronology of the Tripoli diatomite formation (pre-evaporite Messinian, Sicily, Italy). Terra Nova 11, 16–22.

Hilgen, F.J., Krijgsman, W., Langereis, C.G., Lourens, L.J., Santarelli, A., Zachariasse, W.J., 1995. Extending the astronomical (polarity) time scale into the Miocene. Earth and Planetary Science Letters 136, 495–510.

Hilgen, F.J., Abdul Aziz, H., Krijgsman, W., Langereis, C.C., Lourens, L.J., Meulenkamp, E., Raffi, I., Steenbrink, J., Turco, E., van Vugt, N., 1999. Present status of the astronomical (polarity) time-scale for the Mediterranean Late Neogene. Philosophical Transactions of the Royal Society of London 357, 1931–1947.

Hilgen, F.J., Bissoli, L., Iaccarino, S., Krijgsman, W., Meijer, R., Negri, A., Villa, G., 2000. Integrated stratigraphy and astrochronology of the Messinian GSSP at Oued Akrech (Atlantic Morocco). Earth and Planetary Science Letters 182, 237–251.

Hilgen, F.J., Kuiper, K., Krijgsman, W., Snel, E., van der Laan, E., 2007. Astronomical tuning as the basis for high resolution chronostratigraphy: the intricate history of the Messinian Salinity Crisis. Stratigraphy 4, 231–238.

Hilgen, F.J., Lourens, L.J., Van Dam, J.A., 2012. The Neogene Period, from: the Geologic Time Scale 2012. https://doi.org/10.1016/B978-0-444-59425-9.00029-9.

Hsü, K.J., Cita, M.B., Ryan, W.B.F., 1973. The origin of the Mediterranean evaporites. In: Ryan, W.B.F., Hsü, K.J., Dumitrica, P., Lort, J.M., Maync, W., Nesteroff, W.D., Pautot, G., Stradner, H., Wezel, F.C. (Eds.), Initial Reports of the Deep Sea Drilling ProjectVolume XIII. U.S. Government Printing Office, Washington, pp. 1203–1231.

Hsü, K.J., Montadert, L., Bernoulli, D., Cita, M.B., Erikson, A., Garrison, R.E., Kidd, R.B., Melieres, F., Muller, C., Wright, R.H., 1978. Initial report of Deep Sea Drilling Project. Mediterranean Sea42. U.S. Government Printing Office, Washington, DC.

Hüsing, S.K., Kuiper, K.F., Link, W., Hilgen, F.J., Krijgsman, W., 2009. The upper Tortonian–lower Messinian at Monte Dei Corvi (Northern Apennines, Italy): completing a Mediterranean reference section for the Tortonian Stage. Earth and Planetary Science Letters 282, 140–157.

Kastens, K.A., Mascle, J., 1990. The geological evolution of the Tyrrhenian Sea: an introduction to the scientific results of ODP Leg 107. In: Kastens, K.A., Mascle, J. (Eds.), Proceedings of the Ocean Drilling Program, Scientific Results. Ocean Drilling Programvol. 107. College Station, Texas, pp. 3–26.

Kontakiotis, G., Karakitsios, V., Mortyn, P.G., Antonarakou, A., Drinia, H., Anastasakis, G., Agiadi, K., Kafousia, N., De Rafelis, M., 2016. New insights into the early Pliocene hydrographic dynamics and their relationship to the climatic evolution of the Mediterranean Sea. Palaeogeography, Palaeoclimatology, Palaeoecology 459, 348–364.

Kouwenhoven, T., van der Zwaan, G.J., 2006. A reconstruction of late Miocene Mediterranean circulation patterns using benthic foraminifera. Palaeogeography, Palaeoclimatology, Palaeoecology 238, 373–385.

Kouwenhoven, T., Hilgen, F.J., van der Zwaan, G.J., 2003. Late Tortonian-early Messinian stepwise disruption of the Mediterranean-Atlantic connections: constrains from benthic foraminiferal and geochemical data. Palaeogeography, Palaeoclimatology, Palaeoecology 198, 303–319.

Koymans, M.R., van Hinsbergen, D.J.J., Pastor-Galan, D., Vaes, B., Langereis, C.G., 2020. Towards FAIR Paleomagnetic Data Management through Paleomagnetism.org 2.0. Geochemistry, Geophysics, Geosystems 21. https://doi.org/10.1029/2019GC008838.

Krijgsman, W., Hilgen, F.J., Langereis, C.G., Santarelli, A., Zachariasse, W.J., 1995. Late Miocene magnetostratigraphy, biostratigraphy and cyclostratigraphy in the Mediterranean. Earth and Planetary Science Letters 136, 475–494.

Krijgsman, W., Hilgen, F.J., Raffi, I., Sierro, F.J., Wilson, D.S., 1999a. Chronology, causes and progression of the Messinian salinity crisis. Nature 400, 652–655.

Krijgsman, W., Langereis, C.G., Zachariasse, W.J., Boccaletti, M., Moratti, G., Gelati, R., Iaccarino, S., Papani, G., Villa, G., 1999b. Late Neogene evolution of the Taza-Guercif Basin (Rifian Corridor, Morocco) and implications for the Messinian salinity crisis. Marine Geology 153, 147–160.

Krijgsman, W., Hilgen, F.J., Marabini, S., Vai, G.B., 1999c. New paleomagnetic and cyclostratigraphic age constraints on the Messinian of the Northern Apennines (Vena del Gesso Basin, Italy). Memorie della Società Geoligica Italiana 54, 25–33.

Krijgsman, W., Blanc-Valleron, M.-M., Flecker, R., Hilgen, F.J., Kouwenhoven, T.J., Merle, D., Orszag-Sperber, F., Rouchy, J.-M., 2002. The onset of the Messinian salinity crisis in the Eastern Mediterranean (Pissouri Basin, Cyprus). Earth Planet. Sci. Lett. 194, 299–310.

Krijgsman, W., Hilgen, F.J., Langereis, C.G., Zachariasse, W.J., 1994. The age of the Tortonian/Messinian boundary. Earth Planet. Sci. Lett. 121, 533–547.

Krijgsman, W., Fortuin, A.R., Hilgen, F.J., Sierro, F.J., 2001. Astrochronology for the Messinian Sorbas Basin (SE Spain) and orbital (precessional) forcing evaporite cyclicity. Sedimentary Geology 140, 43–60.

Langereis, C.G., Dekkers, M.J., 1992. Paleomagnetisnl and rock magnetism of the Tortonian Messinian boundary stratotype at Falconara, Sicily. Physics of the Earth and Planetary Interiors 71, 100–111.

Laskar, J., Robutel, P., Joutel, F., Gastineau, M., Correia, A.C.M., Levrard, B., 2004. A long term numerical solution for the insolation quantities of the Earth. Astronomy & Astrophysics 428, 261–285.

Lirer, F., Foresi, L.M., Iaccarino, S.M., Salvatorini, G., Turco, E., Cosentino, C., Sierro, F.J., Caruso, A., 2019. Mediterranean Neogene planktonic foraminifer biozonation and biochronology. Earth - Science Reviews 196. https://doi.org/10.1016/j.earscirev.2019.05.013.

Lo Cicero, G., Di Stefano, E., Catalano, R., Sprovieri, R., Agate, M., Contino, A., Greco, G., Mauro, G., 1997. The Ciminna Messinian Evaporitic Basin: Cyclical sedimentation and eustatic control in a transpressive tectonic setting, Field workshop in Western Sicily, June 11–13,1997. Guidebook.

Lofi, J., Gorini, C., Berne, S., Clauzon, G., Tadeu Dos Reis, A., Ryan, W.B.F., Steckler, M.S., 2005. Erosional processes and paleo-environmental changes in the western Gulf of Lions (SW France) during the Messinian salinity crisis. Mar. Geol. 217, 1–30.
Lugli, S., Manzi, V., Roveri, M., Schreiber, B.C., 2010. The Primary Lower Gypsum in the Mediterranean: a new facies interpretation for the first stage of the Messinian salinity crisis. Palaeogeography, Palaeoclimatology, Palaeoecology 297, 83–99.
Malinverno, A., Ryan, W.B., 1986. Extension in the Tyrrhenian Sea and shortening in the Apennines as result of arc migration driven by sinking of the lithosphere. Tectonics 5, 227–245.
Mancini, A.M., Gennari, R., Ziveri, P., Mortyn, P.G., Stolwijk, D.J., Lozar, F., 2020. Calcareous nannofossil and foraminiferal trace element records in the Sorbas Basin: a new piece of the Messinian SalinityCrisis onset puzzle. Paleoceanography and Paleoclimatology 36. https://doi.org/10.1016/j.palaeo.2020.109796.
Manzi, V., Lugli, S., Roveri, M., Schreiber, B.C., 2009. A new facies model for the Upper Gypsum of Sicily (Italy): chronological and palaeoenvironmental constraints for the Messinian salinity crisis in the Mediterranean. Sedimentology 56, 1937–1960.
Manzi, V., Lugli, M., Schreiber, B.C., Gennari, R., 2011. The Messinian "Calcare di Base" (Sicily, Italy) revisited. Geological Society of America Bulletin 123, 347–370.
Manzi, V., Gennari, R., Hilgen, F., Krijgsman, W., Lugli, S., Roveri, M., Sierro, F., 2013. Age refinement of the salinity crisis onset in the Mediterranean. Terra Nova 25, 315–322.
McClelland, J.W., Aliela, I.V., Michener, R.H., 1997. Nitrogen-stable isotope signatures in estuarine food webs: a record of increasing. Urbanization in coastal watersheds. Limnology and Oceanography 42, 930–937.
Meijer, P., 2021. (Paleo)oceanography of semi-enclosed seas with a focus on the Mediterranean region; Insights from basic theory. Earth-Science Reviews 221. https://doi.org/10.1016/j.earscirev.2021.103810.
Meisch, C., 2000. Freshwater Ostracoda of Western and Central Europe. Spektrum Aakademischer Verlag, Berlin, pp. 1–522.
Meyer, J., Wrozyna, C., Gross, M., Leis, A., Piller, W.E., 2016. Morphological and geochemical variations of Cyprideis (Ostracoda) from modern waters of the northern Neotropics. Limnology https://doi.org/10.1007/s10201-016-0504-9.
Milker, Y., Schmiedl, G., 2011. A taxonomic guide to modern benthic foraminifera of the western Mediterranean Sea. Palaeontologia Electronica 15, 1–134.
Morigi, C., Negri, A., Giunta, S., Kouwenhoven, T., Krijgsman, W., Blanc-Valleron, M.-M., Orszag-Sperber, F., Rouchy, J.-M., 2007. Integrated quantitative biostratigraphy of the latest Tortonian–early Messinian Pissouri section (Cyprus): an evaluation of calcareous plankton bioevents. Geobios 40, 267–279.
Natalicchio, M., Pellegrino, L., Clari, P., Pastero, L., dela Pierre, F., 2021. Gypsum Lithofacies and Stratigraphic Architecture of a Messinian Marginal Basin (Piedmont Basin, NW Italy). Sedimentary Geology https://doi.org/10.1016/j.sedgeo.2021.106009.
Neale, J.W., 1988. Ostracods and palaeosalinity reconstruction. In: De Deckker, P., Colin, J.-P., Peypouquet, J.P. (Eds.), Ostracoda in the Earth Science. Elsevier, Amsterdam, pp. 125–155.
Ochoa, D., Sierro, F.J., Lofi, J., Maillard, A., Flores, J.A., Suárez, M., 2015. Synchronous onset of the Messinian evaporite precipitation: first Mediterranean offshore evidence. Earth and Planetary Science Letters 427, 112–124.
Patacca, E., Sartori, R., Scandone, P., 1990. Tyrrhenian basin and Apenninic arcs: kinematic relations since late Tortonian times. Memorie della Societa Geologica Italiana 45, 425–451.
Pellegrino, L., Natalicchio, M., Abe, K., Jordan, R.W., Favero Longo, S., Ferrando, S., Carnevale, G., Dela Pierre, F., 2021. Tiny, glassy and rapidly trapped: the nano-sized planktonic diatoms in Messinian gypsum. Geology 49. https://doi.org/10.1130/G49342.1.
Perch-Nielsen, K., 1985. Cenozoic calcareous nannofossils. In: Bolli, H.M., Sanders, J.B., Perch-Nielsen, K. (Eds.), Plankton Stratigraphy. Cambridge University Press, Cambridge, pp. 427–554.
Perri, E., Gindre-Chanu, L., Caruso, A., Fefala, M., Scopelliti, G., Tucker, M., 2017. Microbial-mediated pre-salt carbonate deposition during the Messinian salinity crisis (Calcare di Base fm., Southern Italy). Marine and Petroleum Geology 88, 235–250.
Raad, F., Lofi, J., Maillard, A., Tzevahirtzian, A., Caruso, A., 2021. The Messinian Salinity Crisis deposits in the Balearic Promontory: an undeformed analog of the MSC Sicilian basins?? Marine and Petroleum Geology 124, 1–20.
Raad, F., Ebner, R., Heida, H., Meijer, P., Lofi, J., Maillard, A., Garcia-Castellanos, D., 2022. A song of volumes, surfaces and fluxes: the case study of the Central Mallorca Depression (Balearic Promontory) during the Messinian Salinity Crisis. Basin Research 00, 1–27.
Raffi, I., Mozzato, C.A., Fornaciari, E., Hilgen, F.J., Rio, D., 2003. Late Miocene calcareous nannofossil biostratigraphy and astrobiochronology for the Mediterranean region. Micropaleontology 49, 1–26.
Rausch, L., Stoica, M., Lazarev, S., 2021. A late miocene – early pliocene paratethyan type ostracod fauna from the Denizli basin (sw anatolia) and its palaeogeographic implications. Acta Palaeontologica Romaniae 16, 3–56.
Rouchy, J.M., 1982. La génèse des évaporites messiniennes de Méditerranée. Bulletin du Muséum National d'Histoire Naturelle. Sciences de la Terre, Paris, pp. 1–280.
Rouchy, J.M., Caruso, A., 2006. The Messinian salinity crisis in the Mediterranean basin: a reassessment of the data and an integrated scenario. Sedimentary Geolgy 188, 35–67.
Rouchy, J.M., Taberner, C., Blanc-Valleron, M.M., Sprovieri, R., Russell, M., Pierre, C., Di Stefano, E., Pueyo, J.J., Caruso, A., Dinarès-Turell, J., Gomis-Coll, E., Wolff, G.A., Cespuglio, G., Ditchfiels, P., Pestrea, S., Combourieu-Nebout, N., Santisteban, C., Grimalt, J.O., 1998. Sedimentary and diagenetic markers of the restriction in a marine basin: the Lorca Basin (SE Spain) during the Messinian. Sedimentary Geology 121, 23–55.
Roure, F., Howell, D.G., Muller, C., Moretti, I., 1990. Late Cenozoic subduction complex of Sicily. Journal of Structural Geology 12, 259–266.
Roveri, M., Lugli, S., Manzi, V., Scheiber, B.C., 2008a. The Messinian Sicilian stratigraphy revisited: new insights for the Messinian salinity crisis. Terra Nova 20, 483–488.
Roveri, M., Lugli, S., Manzi, V., Schreiber, B.C., 2008b. The shallow- to deep-water record of the Messinian Salinity Crisis: new insights from Sicily, Calabria and Apennine basins. In: Briand, F. (Ed.), the Messinian Salinity Crisis mega-deposits to microbiology – a consensus report. CIESM Workshop Monographs,33, Monaco, pp. 73–82.
Roveri, M., Flecker, R., Krijgsman, W., Lofi, J., Lugli, S., Manzi, V., Sierro, F.J., Bertini, A., Camerlenghi, A., De Lange, G., Govers, R., Hilgen, F.J., Hubscher, C., Meijer, P.T., Stoica, M., 2014. The Messinian Salinity Crisis: past and future of a great challenge for marine sciences. Marine Geology 352, 25–58.
Roveri, M., Manzi, V., Lugli, S., Schreiber, B.C., Caruso, A., Rouchy, J.M., Iaccarino, S.M., Gennari, R., Vitale, F.P., Ricci Lucchi, F., 2006. Clastic vs. primary precipitated evaporites in the Messinian Sicilian basins. RCMNS IC Parma 2006 "the Messinian salinity crisis revisited II" post-congress field-trip. Acta Nat. L'Ateneo Parmen. 42, 125–199.
Ruggieri, G., Sprovieri, R., 1978. The "desiccation theory" and its evidences in Italy and in Sicily. Memorie della Societa Geologica Italiana 16, 165–169.
Ryan, W., 2009. Decoding the Mediterranean salinity crisis. Sedimentology 56, 95–136.
Sciuto, F., Baldanza, A., 2020. Full restoration of marine conditions after the late Messinian Mediterranean Lago-Mare phase in Licodia Eubea and Villafranca Tirrena areas (East Sicily). Carnets de géologie 20, 107–123.
Sengör, A.M.C., 1979. Mid-Mesozoic closure of Permo-Triassic Tethys and its implications. Nature 279, 590–593.
Shackleton, M., Hall, M., 1997. The late Miocene stable isotope record, site 9261. Environmental Science, Geography https://doi.org/10.2973/odp.proc.sr.154.119.1997.
Sierro, F.J., Flores, J.C., Civis, J., Gonza´lez Delgado, J.A., Francés, G., 1993. Late Miocene globorotalid event-stratigraphy and biogeography in the NE-Atlantic and Mediterranean. Marine Micropaleontology 21, 143–168.
Sierro, F.J., Hilgen, F.J., Krijgsman, W., Flores, J.A., 2001. The Abad composite (SE Spain): a Mediterranean and global reference sec-tion for the Messinian. Palaeogeography, Palaeoclimatology, Palaeoecology 168, 141–169.
Sprovieri, R., Di Stefano, E., Caruso, A., Bonomo, S., 1996. High resolution stratigraphy in the Messinian Tripoli Formation in Sicily. Paleopelagos 6, 415–435.
Stoica, M., Lazar, I., Krijgsman, W., Vasiliev, I., Jipa, D., Floroiu, A., 2013. Paleoenvironmental evolution of the East Carpathian foredeep during the late Miocene-early Pliocene (Dacian Basin; Romania). Global and Planetary Change 103, 135–148.
Stoica, M., Krijgsman, W., Fortuin, A., Gliozzi, E., 2016. Paratethyan ostracods in the Spanish Lago-Mare: more evidence for interbasinal exchange at high Mediterranean sea-level. Palaeogeography, Palaeoclimatology, Palaeoecology 441, 854–870.
Tzevahirtzian, A., Caruso, A., Scopelliti, G., Baudin, F., Blanc-Valleron, M.-M., 2022. Onset of the Messinian Salinity Crisis: Sedimentological, petrographic and geochemical characterization of the pre-salt sediments from a new core (Caltanissetta Basin, Sicily). Marine and Petroleum Geology 141. https://doi.org/10.1016/j.marpetgeo.2022.105686.
Vai, G.B., 1997. Cyclostratigraphic estimate of the Messinian stage duration. In: Montanari, A., Odin, G.S., Coccioni, R. (Eds.), Miocene Stratigraphy - An Integrated Approach. Elsevier, pp. 461–474.
Van Couvering, J.A., Castradori, D., Cita, M.B., Hilgen, F.J., Rio, D., 2000. The base of the Zanclean Stage and of the Pliocene Series. Episodes 23, 179–187.
van der Laan, E., Snel, E., de Kaenel, E., Hilgen, F.J., Krijgsman, W., 2006. No major deglaciation across the Miocene-Pliocene boundary: integrated stratigraphy and astronomical tuning of the Loulja sections (Bou Regreg area, NW Morocco). Paleoceanography 21. https://doi.org/10.1029/2005PA001193.
Vidal, L., Bickert, T., Wefer, G., Roehl, U., 2002. Late Miocene stable isotope stratigraphy of SE Atlantic ODP Site 1085: Relation to Messinian events. Marine Geology 180, 71–78.
Zachariasse, W.J., Kontakiotis, G., Lourens, L.J., Antonarakou, A., 2021. The Messinian of Agios Myron (Crete, Greece): a key to better understanding of diatomite formation on Gavdos (south of Crete). Palaeogeography, Palaeoclimatology, Palaeoecology 581. https://doi.org/10.1016/j.palaeo.2021.110633.
Zachariasse, W.J., Lourens, L.J., 2021. The Messinian on Gavdos (Greece) and the status of currently used ages for the onset of the MSC and gypsum precipitation. Newsletters on Stratigraphy https://doi.org/10.1127/nos/2021/0677.